



G4 - STAINLESS STEEL

- Group members:
- Akshita Mittal
- Sanket Muthal
- Sejal Kotian
- Sohail Shaikh
- Yash Kumar

TOPICS TO DISCUSS

- Stainless Steel- types
- What are processing maps?
- Identification of flow instabilities in the processing maps of AISI 304 stainless steel
- 316L Stainless Steel
- 316LN Stainless Steel
- Laser Forming of Metals



STAINLESS STEEL

- **Stainless steel**, originally called **rustless steel**, belongs to the group of **ferrous alloys** that contain a minimum of approx. **11% chromium**, which prevents the iron from **rusting** and also provides heat-resistant properties.
- Different types of stainless steel include the elements **carbon**, **nitrogen**, aluminium, silicon, sulphur, titanium, nickel, copper, selenium, niobium, and molybdenum.
- Specific types of stainless steel are often designated by their **AISI** three-digit number for example, **304 stainless**.
- **Resistance to corrosion** and staining, **low maintenance**, and **lustre** make stainless steel an ideal material for many applications where both the **strength of steel** and **corrosion resistance** are required.
- The addition of **nitrogen** also improves resistance to pitting corrosion and increases mechanical strength.
- Thus, there are numerous grades of stainless steel with varying chromium and molybdenum contents to suit the environment the alloy must endure.

TYPES OF STAINLESS STEEL

- Five main families, based on crystalline structure:
 1. Austenitic
 2. Ferritic
 3. Martensitic
 4. Duplex
 5. Precipitation Hardening
- Austenitic Steel - largest family, making up around 2/3rds of all stainless steel production
- Austenitic Stainless steels are further subdivided into two sub-groups - 200 and 300 series.
- 200 series - Chromium- Manganese- Nickel alloy that maximise the use of Mn and N to minimise the use of Nickel. Due to their nitrogen addition, they possess approximately 50% higher yield strength than 300 series stainless sheets of steel.

- 300 series are chromium-nickel alloys. They are the largest group and the most widely used.
 - Type [304](#): The best-known grade is Type 304, also known as 18/8 and 18/10 for its composition of 18% chromium and 8% or 10% nickel, respectively.
 - Type [316](#): The second most common austenitic stainless steel is Type 316. The addition of 2% **molybdenum** provides greater resistance to acids and localised corrosion caused by chloride ions. Low-carbon versions, such as [316L](#) or 304L, have carbon contents below 0.03% and are used to avoid corrosion problems caused by welding.

WHAT ARE PROCESSING MAPS?

- A processing map is an explicit representation of the response of a material to the imposed process parameters, in terms of microstructural mechanisms.
- It consists of a superimposition of a *power dissipation map* and an *instability map*. These are developed on the basis of the Dynamic Materials Model (DMM).
- Power Dissipation Map
 - At a given temperature in the hot working regime, the rate of dissipation work (power) is directly proportional to the rate of internal entropy production which is always positive since the process is irreversible.
 - Total Rate of entropy production = Conduction Entropy + Microstructural Dissipation (dislocation movement)

$$P = \int_0^{\dot{\varepsilon}} \bar{\sigma} \cdot d\dot{\varepsilon} + \int_0^{\dot{\bar{\sigma}}} \dot{\bar{\varepsilon}} \cdot d\bar{\sigma} = G + J$$

- the first integral is called G content and the second one a J co-content since it is a complementary part of G content.
- We further define the efficiency of power dissipation with respect to a linear dissipator ($m=1$)

$$\frac{\Delta J / \Delta P}{(\Delta J / \Delta P)_{linear}} = \frac{m/(m+1)}{1/2} = \frac{2m}{m+1} \equiv \eta \quad (9)$$

WHAT ARE PROCESSING MAPS?

- **Instability Map**
- The stability condition described in the Dynamic Materials Model is that considered by Ziegler.
- $$\xi(\dot{\varepsilon}) = \frac{\partial \ln(m / m + 1)}{\partial \ln \dot{\varepsilon}} + m > 0$$
- The well known manifestations of flow instabilities are adiabatic shear bands, flow localization, dynamic strain aging (Lüder's bands), kink bands, mechanical twinning and flow rotations.
- **Processing Map**
- Each of the domains in the processing map represents a microstructural mechanism that contributes to the power dissipation and is deterministic in the sense that kinetic laws are obeyed.
- **Hot Deformation Mechanisms**
 - Dynamic Recrystallization (DRX)
 - Superplastic Deformation:
 - Dynamic Recovery:
 - Wedge Cracking:

WHAT ARE PROCESSING MAPS?

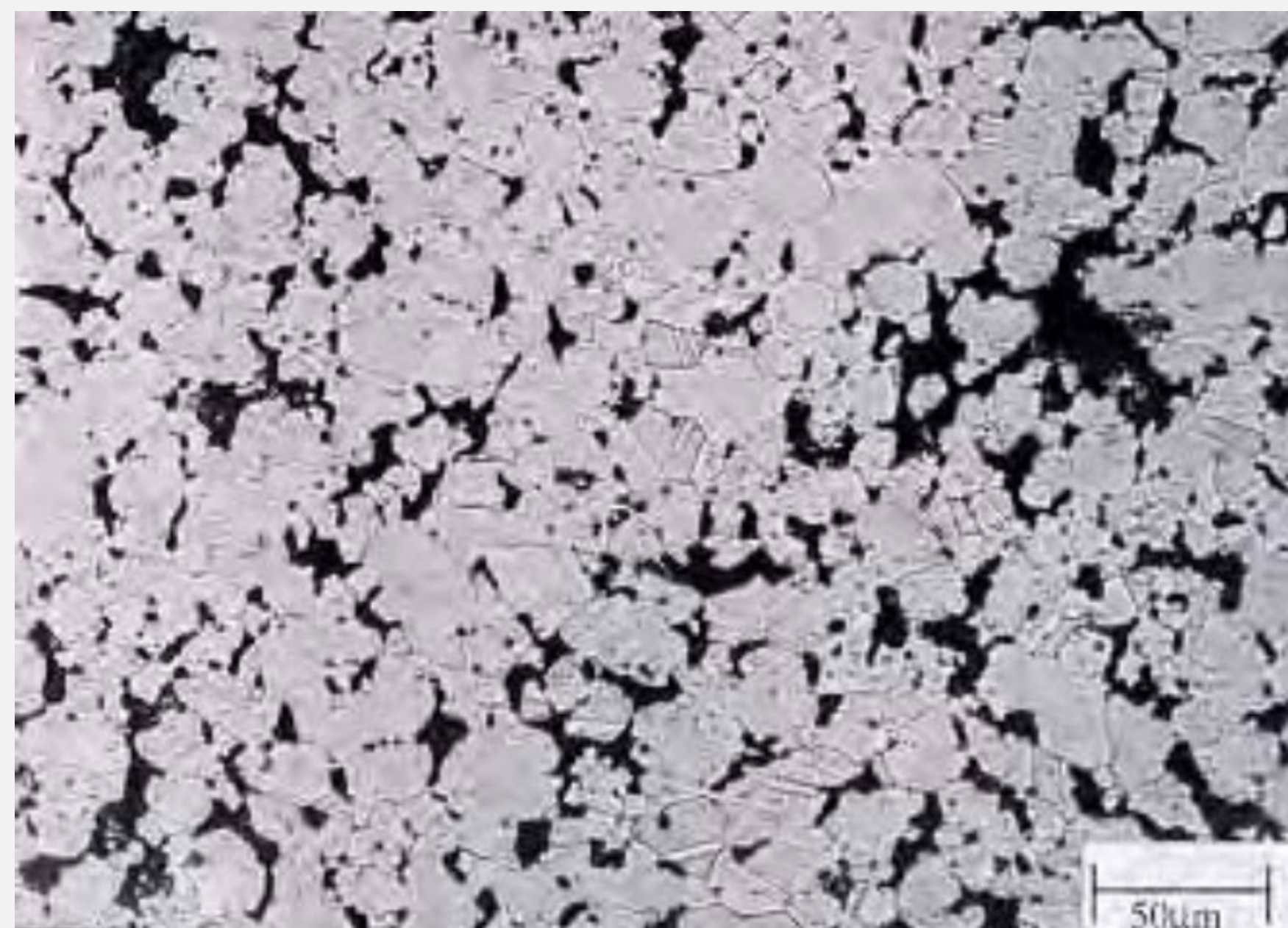
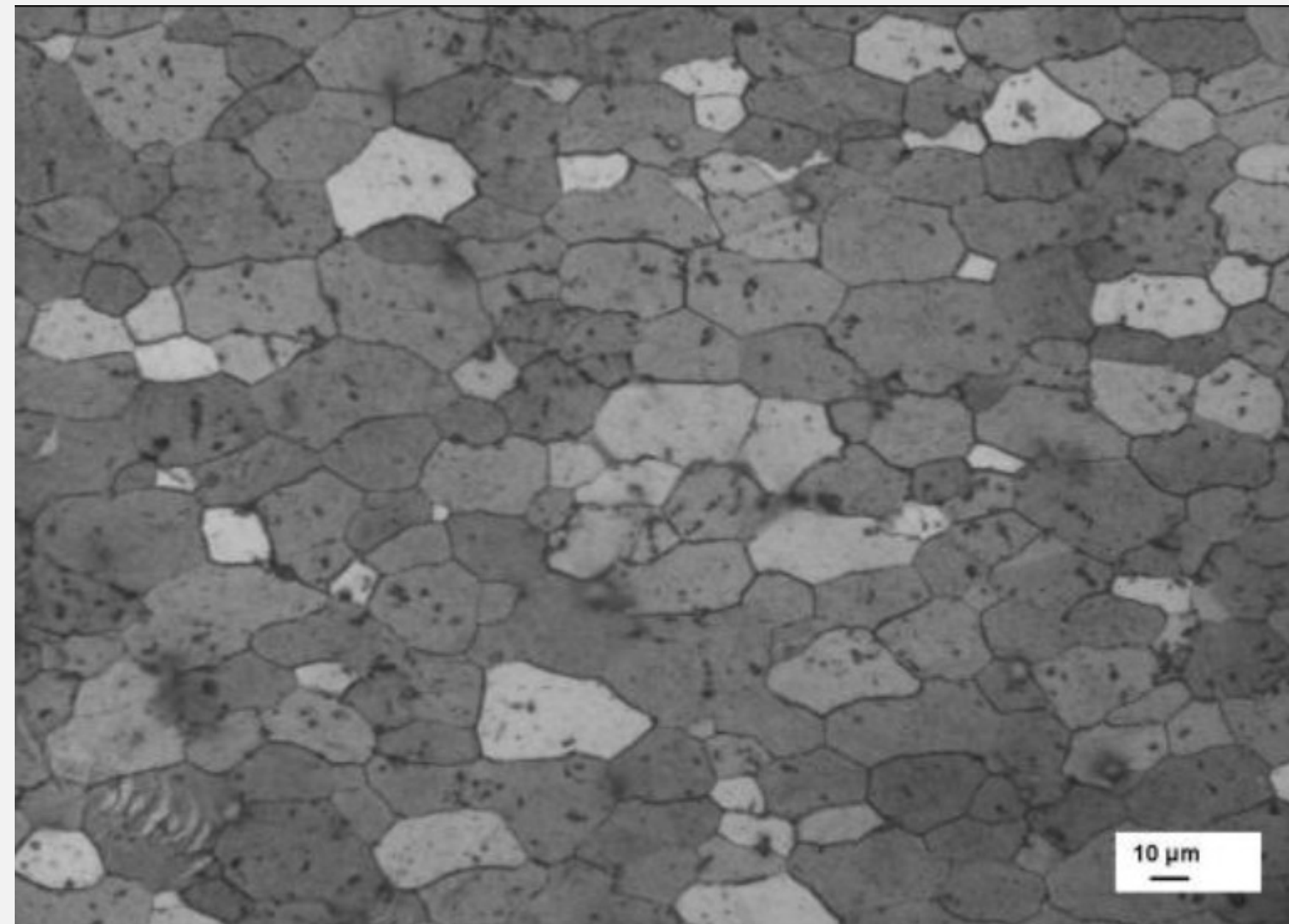
- **Processing Map**
- Each of the domains in the processing map represents a microstructural mechanism that contributes to the power dissipation and is deterministic in the sense that kinetic laws are obeyed.
- **Hot Deformation Mechanisms**
 - Dynamic Recrystallization (DRX)
 - Superplastic Deformation
 - Dynamic Recovery
 - Wedge Cracking
 - Void Formation
 - Inter-crystalline Cracking
 - Flow Instability Processes

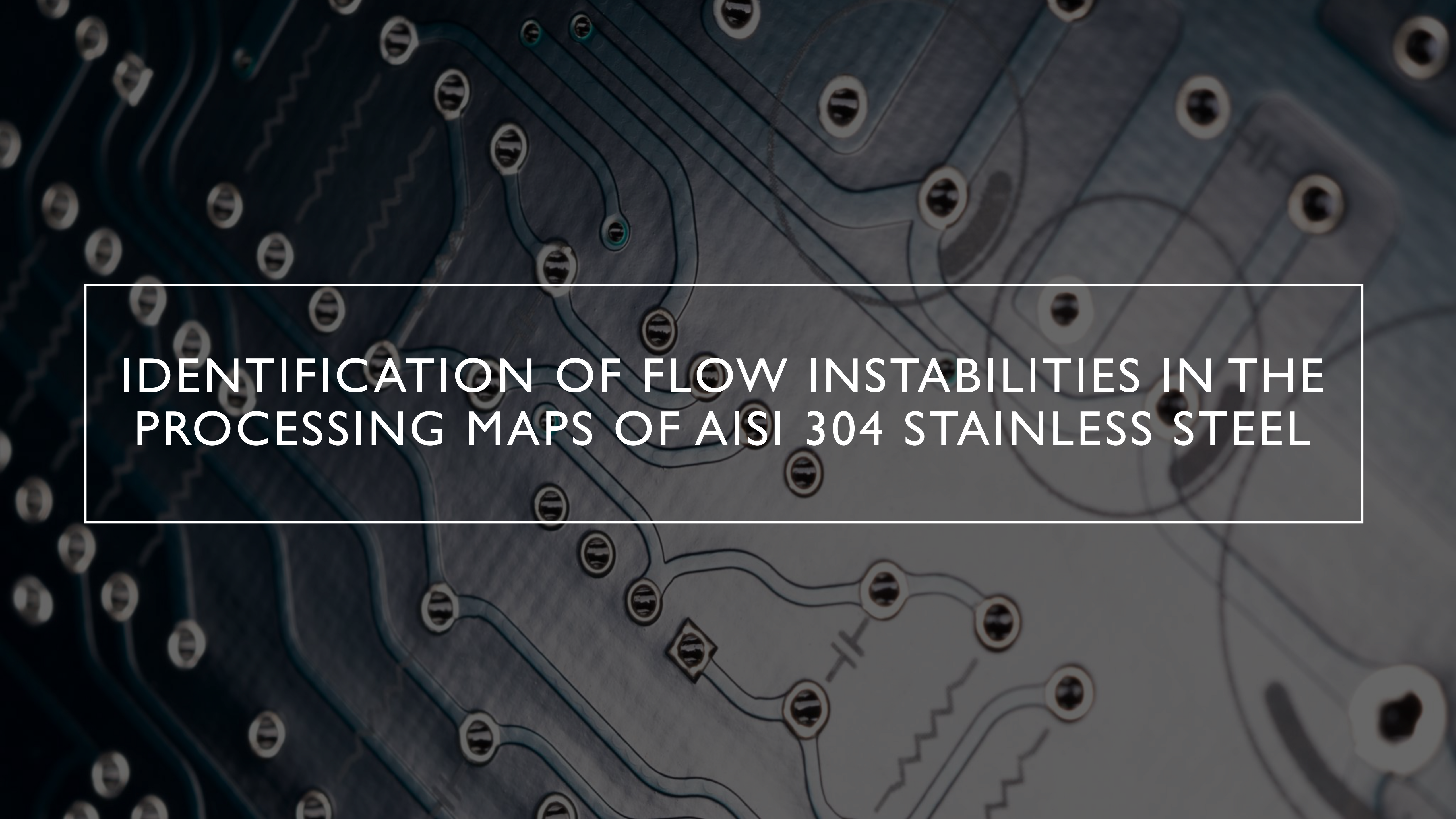
- **DRX:** DRX domain generally occurs in the homologous temperature range 0.7-0.8 and at intermediate strain rates ($0.1-1 \text{ s}^{-1}$) in the maps for low stacking fault energy materials. The strain rate range is lower- 1 for high stacking fault energy materials ($0.01-0.001 \text{ s}^{-1}$).
- The maximum efficiency of power dissipation in the DRX domain is about 30-40% for low stacking fault energy materials (Ni, Cu, Zn, Ti, Zr-base alloys) and is about 50-55% in high stacking fault energy materials (Al and Cd).
- The contours in the DRX domain are widely spaced representing a less steep hill and present a fairly wide window in most materials.
- The grain boundaries in the DRX microstructure are wavy in nature.



- **Superplasticity/Wedge Cracking Domain**

- The super-plasticity/wedge cracking domain occurs at temperatures of $0.7\text{-}0.8 T_m$ and strain rates lower than 0.01 s^{-1} .
- Both processes are characterized by a **high efficiency of power dissipation** ($> 60\%$)
- steep rise in efficiency with decrease in strain rate (contours in the map occur closer).
- If the domain represents super-plasticity, the tensile ductility will be abnormally high (several hundreds of percent) at the temperature and strain rate corresponding to the peak efficiency, but will be poor if wedge cracking occurs.

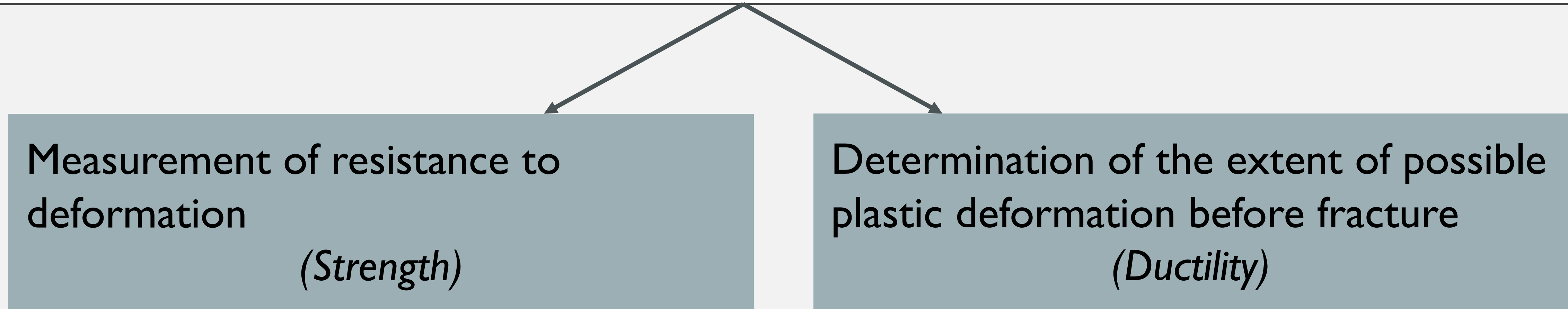




IDENTIFICATION OF FLOW INSTABILITIES IN THE PROCESSING MAPS OF AISI 304 STAINLESS STEEL

INTRODUCTION

EVALUATION OF WORKABILITY



*“Measurement and prediction of limit of
deformation before fracture.”*

To define the processing windows in the desired range of strain rates, workability parameters should be optimum in the specified temperature domain.

WORKABILITY PARAMETERS

$$\Sigma = F(\epsilon, \dot{\epsilon}, T)$$

The strain rate sensitivity parameter,

$$m = \frac{\partial \ln \sigma}{\partial \ln \dot{\epsilon}} \quad (2)$$

The flow-softening rate,

$$\gamma = \frac{1}{\sigma} \frac{\partial \sigma}{\partial \epsilon} = \frac{\partial \ln \sigma}{\partial \epsilon} \quad (3)$$

The flow localization parameter for plane strain compression
[3–5]

$$\alpha = \frac{-\gamma}{m} \quad (4)$$

The temperature sensitivity of flow stress,

$$s = \frac{1}{T} \frac{\partial \ln \sigma}{\partial (1/T)} \quad (5)$$

The efficiency of power dissipation [32],

$$\eta = \frac{J}{J_{\max}} = \frac{P - G}{J_{\max}} = 2 \left[1 - \frac{1}{\sigma \dot{\epsilon}} \int_0^{\dot{\epsilon}} \sigma d\dot{\epsilon} \right] \quad (6)$$

The intrinsic hot workability parameter [12],

$$\varsigma = \frac{\dot{W}_H}{\dot{W}_{H_{\min}}} - 1 = \frac{2}{\sigma \dot{\epsilon}} \int_0^{\dot{\epsilon}} \sigma d\dot{\epsilon} - 1 \quad (7)$$

MATERIAL FLOW INSTABILITIES DURING HOT DEFORMATION

- On the basis of Raj maps, the deformation characteristics of materials are interpreted as follows.
- In the low temperature ($T \leq 0.25T_m$), high strain rate regime ($10\text{--}100 \text{ s}^{-1}$), void formation occurs at hard particles leading to ductile fracture.
- In the high temperature ($T \geq 0.75T_m$), low strain rates ($\leq 10\text{--}3 \text{ s}^{-1}$) regime, wedge cracking caused by grain boundary sliding occurs (except in superplastic materials in which wedge cracking is at a minimum).
- In high temperature ($T_m \approx 0.75$) and high strain rate regime ($10\text{--}1$ to 10 s^{-1}), dynamic recrystallization occurs in low stacking fault energy materials.
- At very high strain rates ($\geq 10 \text{ s}^{-1}$) there is a possibility for the occurrence of adiabatic shear bands and these lead to flow localization.
- Out of all the above mechanisms, DRX and superplastic deformation are ‘safe’ mechanisms for hot working while dynamic recovery is preferred for warm working. All other mechanisms either cause microstructural damage or inhomogeneities of varying intensities and hence are to be avoided in the microstructure of the component

INSTABILITY CRITERION

- 1.Flow localization criterion
- 2.Gegel's stability criterion
- 3.Alexander's stability criterion
- 4.Instability criterion based on Ziegler's plastic flow theory

GEGEL'S AND ALEXANDER'S FLOW INSTABILITY CRITERION

$$0 < m \leq 1 \quad (10)$$

$$\frac{\partial \eta}{\partial(\ln \dot{\varepsilon})} < 0 \quad (11)$$

$$s \geq 1 \quad (12)$$

$$\frac{\partial s}{\partial(\ln \dot{\varepsilon})} < 0 \quad (13)$$

From Eq. (11), a relation between η and m for stable material flow can be written as

$$\frac{2m}{m + 1} < \eta \quad (14)$$

Using Eq. (5) the stability condition (13) can be written in form

$$\Rightarrow \frac{\partial m}{\partial T} > 0 \quad (15)$$

$$0 < m \leq 1 \quad (10)$$

$$\frac{\partial m}{\partial(\ln \dot{\varepsilon})} < 0 \quad (11)$$

$$s \geq 1 \quad (12)$$

$$\frac{\partial s}{\partial(\ln \dot{\varepsilon})} < 0 \quad (13)$$

From Eq. (11), a relation between η and m for stable material flow can be written as

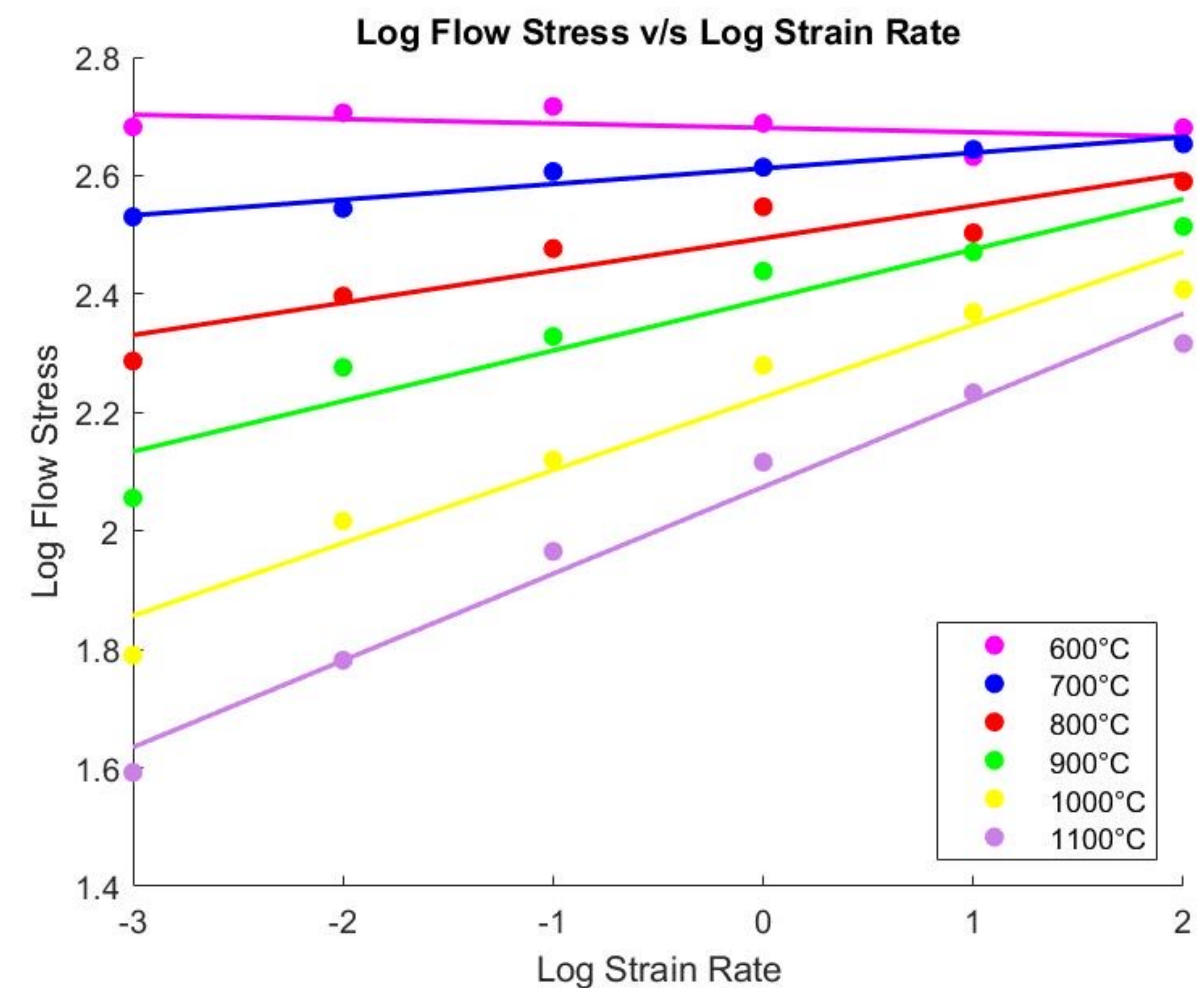
$$\frac{2m}{m + 1} < \eta \quad (14)$$

Using Eq. (5) the stability condition (13) can be written in form

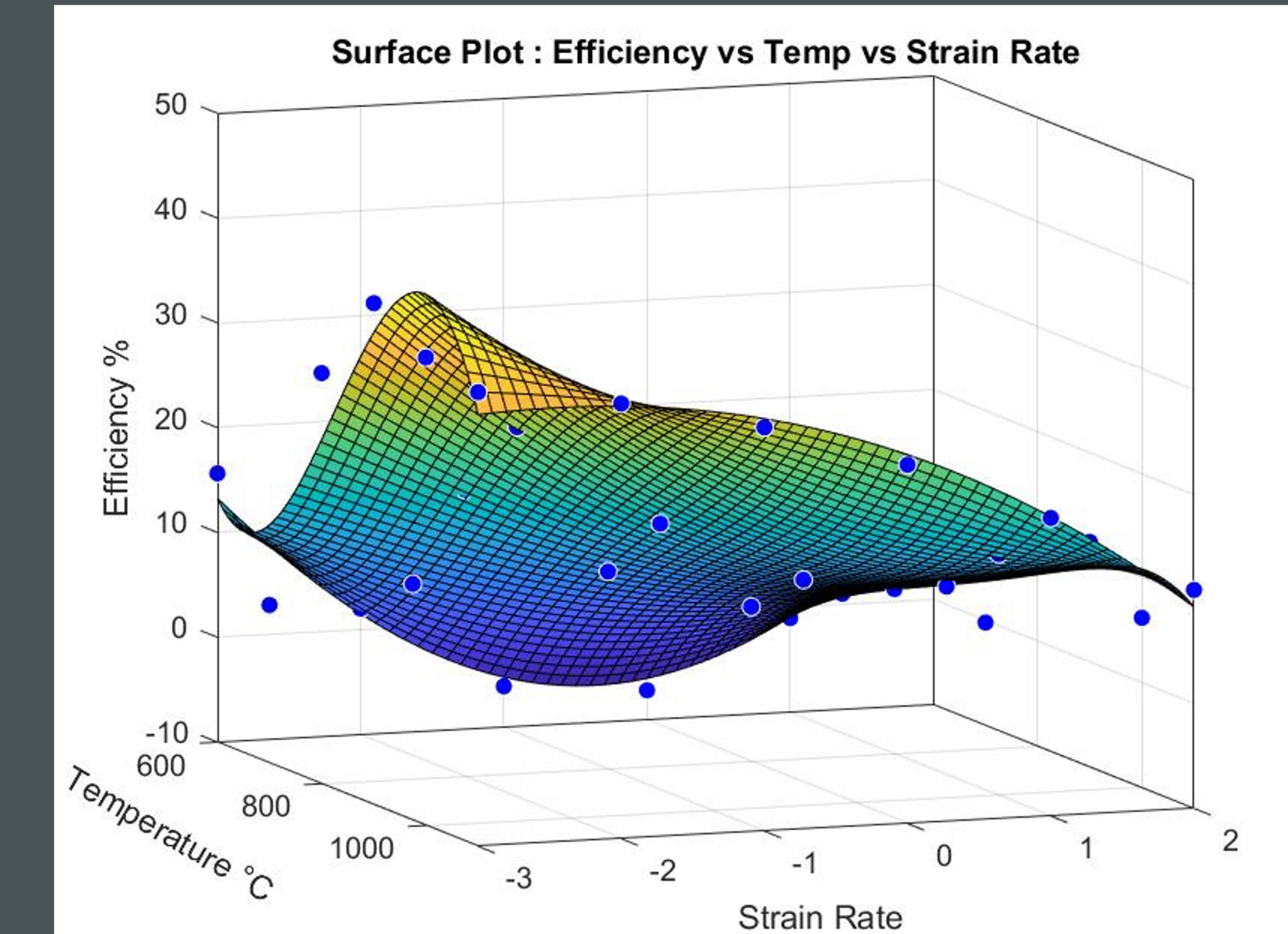
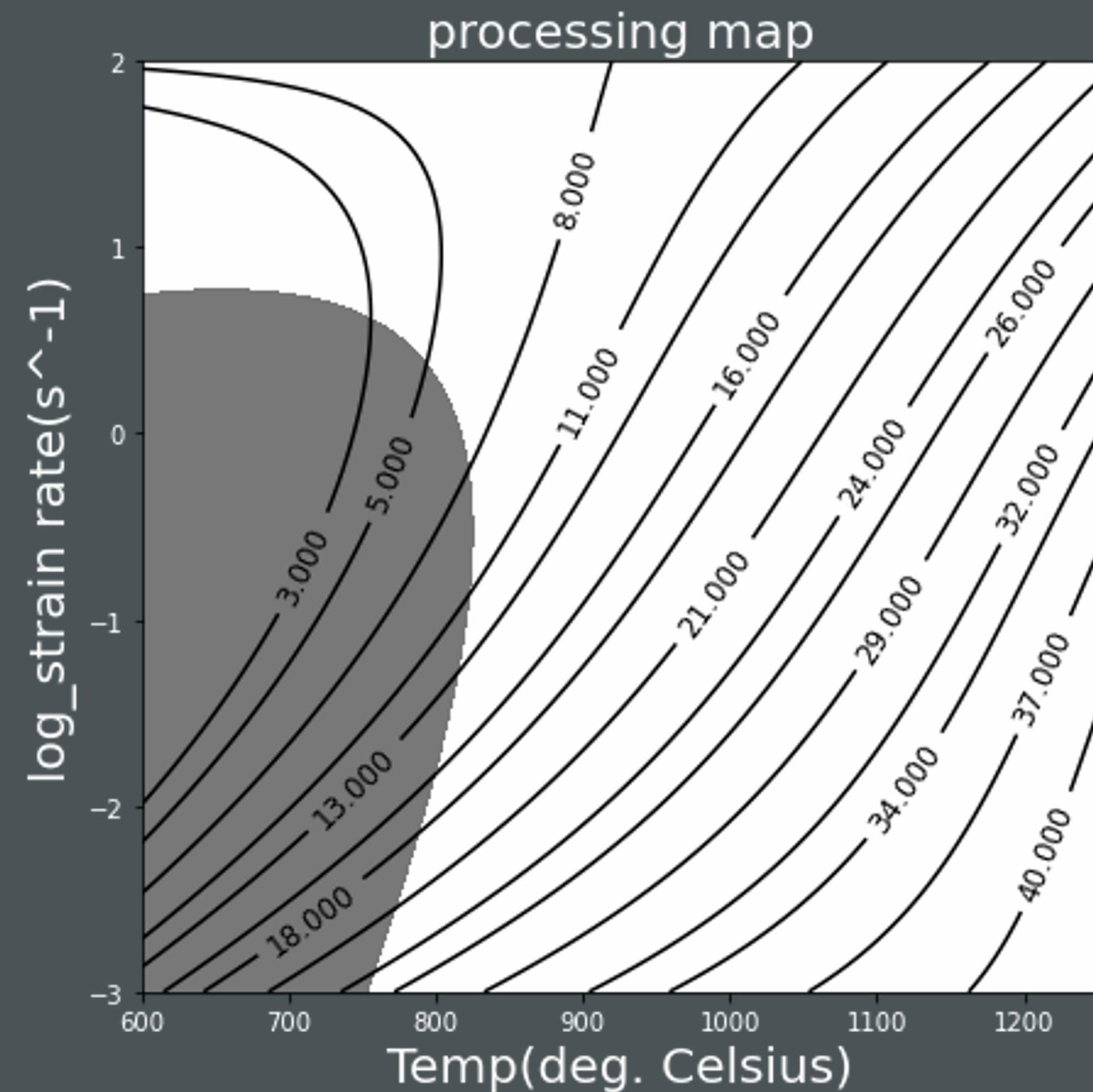
$$\Rightarrow \frac{\partial m}{\partial T} > 0 \quad (15)$$

INSTABILITY CRITERION BASED ON ZIEGLER'S PLASTIC FLOW THEORY

$$\xi(\dot{\varepsilon}) = \frac{\partial \{\ln[m/(m+1)]\}}{\partial (\ln \dot{\varepsilon})} + m < 0$$



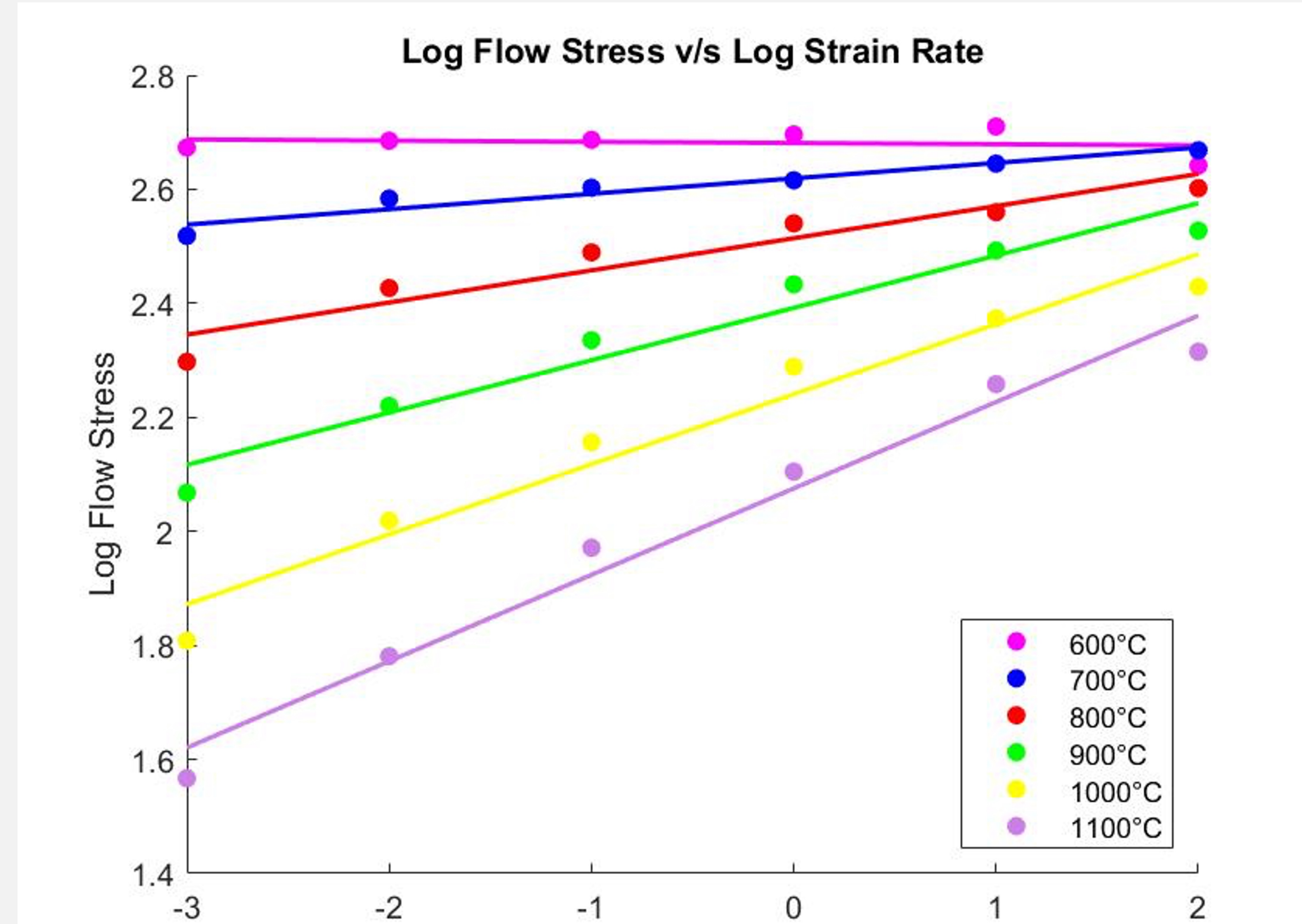
. Variation of flow stress with strain rate for as-cast AISI 304 stainless steel at a strain rate of 0.5



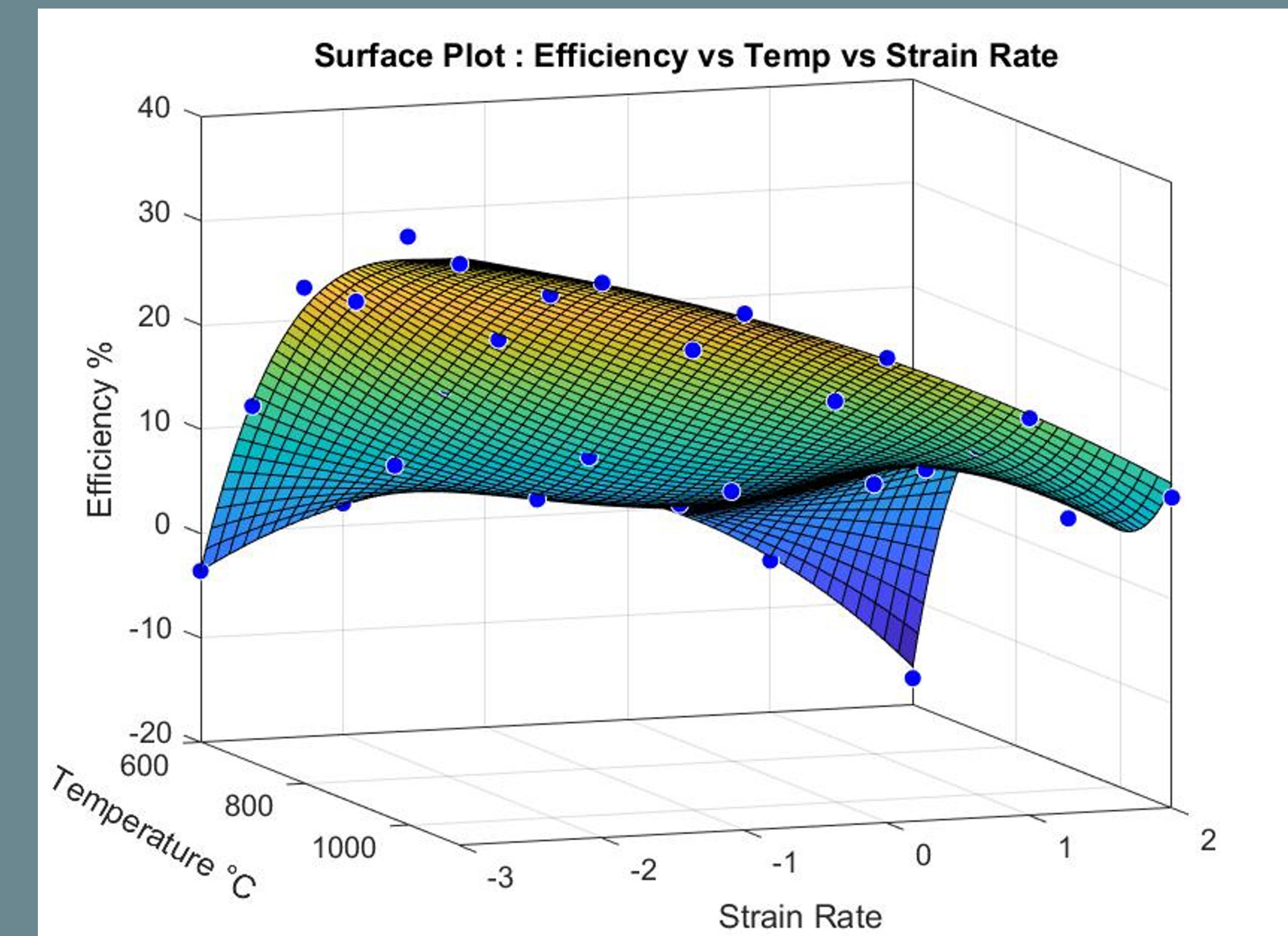
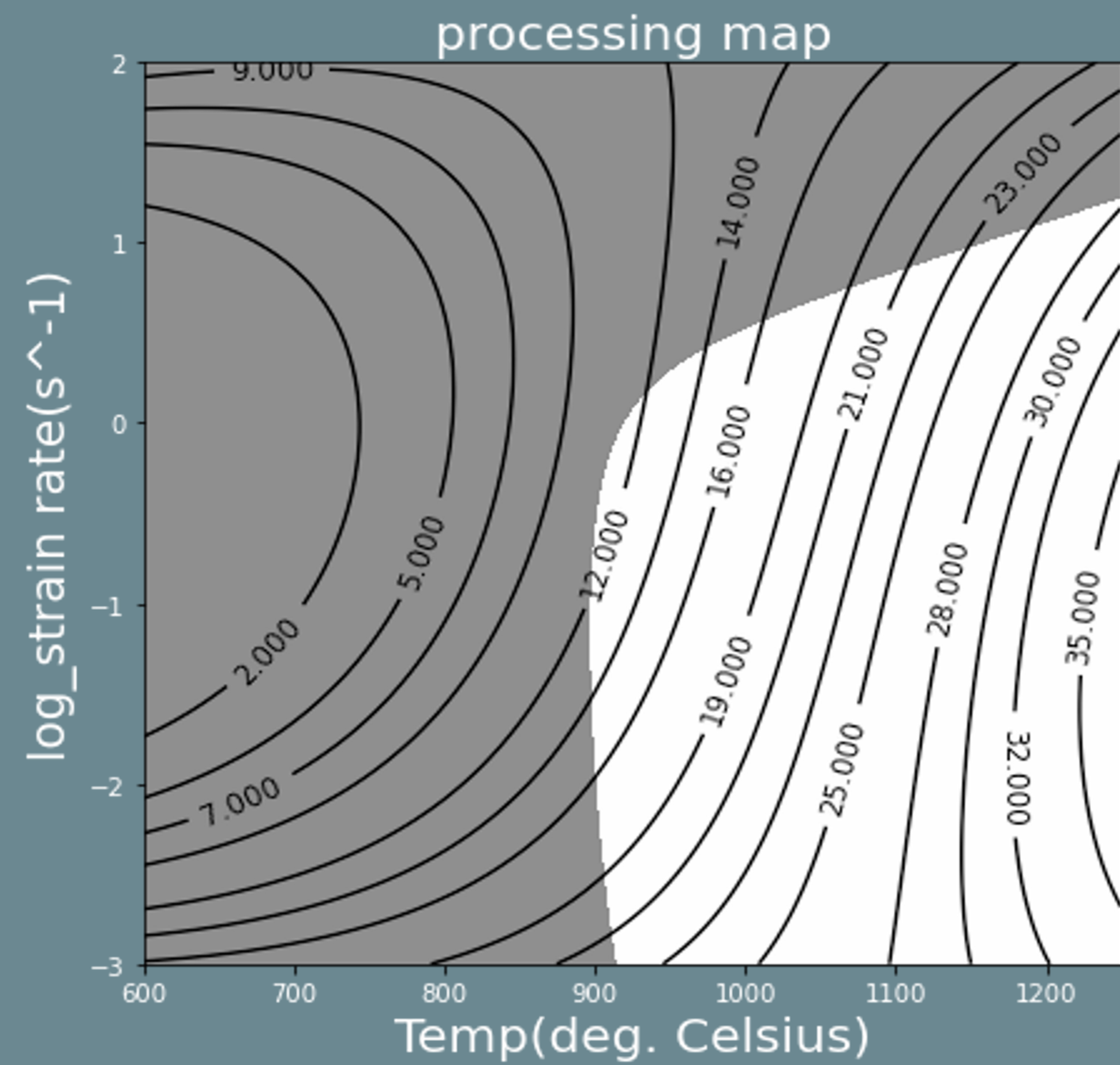
PROCESSING MAP FOR AS- CAST AISI 304 COMMERCIAL STAINLESS STEEL AT A STRAIN OF 0.5. CONTOUR NUMBERS REPRESENT PERCENT EFFICIENCY OF POWER DISSIPATION. SHADED REGION CORRESPONDS TO FLOW INSTABILITY.

Manifestation	Temperature, °C	Strain rate, s⁻¹
Dynamic recrystallization	1000-1250	0.001-1
Flow instability	600-750	0.001-10
Optimum Conditions: 1250°C and 0.001 s⁻¹		

METALLURGICAL INTERPRETATION AND PROCESSING
CONDITIONS FOR AS-CAST COMMERCIAL 304
STAINLESS STEEL



Variation of flow stress with strain rate for as-cast AISI 304 stainless steel at a strain rate of 0.5



Processing map for wrought AISI 304 commercial stainless steel at a strain of 0.5. Contour numbers represent percent efficiency of power dissipation. Shaded region corresponds to flow instability.

Manifestation	Temperature, °C	Strain rate, s⁻¹
Dynamic recrystallization	850-1250	0.001-1
Flow localization	600-900 950-1250	> 0.001 > 1
Optimum Conditions: 1100°C and 0.01 s⁻¹		

METALLURGICAL INTERPRETATION AND PROCESSING
CONDITIONS FOR WROUGHT AISI 304 COMMERCIAL
STAINLESS STEEL

COMPARISON OF THE VARIOUS EXISTING INSTABILITY THEORIES WITH THE REPORTED MICROSTRUCTURAL OBSERVATIONS ON AISI 304 AS CAST STAINLESS STEEL

T (°C)	Strain rate $\dot{\varepsilon}$ (s ⁻¹)	Flow localization theory Eq. (31)	Gegel's instability theory Eqs. (32)–(35)	Alexander's instability theory Eqs. (36)–(39)	Simplified instability theory Eq. (40)	Instability theory due to PRM Eq. (42)	Microstructural observations
600	0.001	Unstable	Unstable	Unstable	Unstable	Unstable	Flow localization
600	1.0	Unstable	Unstable	Unstable	Unstable	Unstable	Flow localization
1000	0.001	Stable	Unstable	Unstable	Stable	Stable	Dynamic recrystallization
1100	0.01	Stable	Unstable	Unstable	Stable	Stable	Dynamic recrystallization
1100	100	Stable	Unstable	Unstable	Unstable	Stable	Dynamic recovery
1200	0.001	Stable	Unstable	Unstable	Stable	Stable	Dynamic recrystallization
1200	0.1	Stable	Unstable	Unstable	Stable	Stable	Dynamic recrystallization



316L STAINLESS STEEL

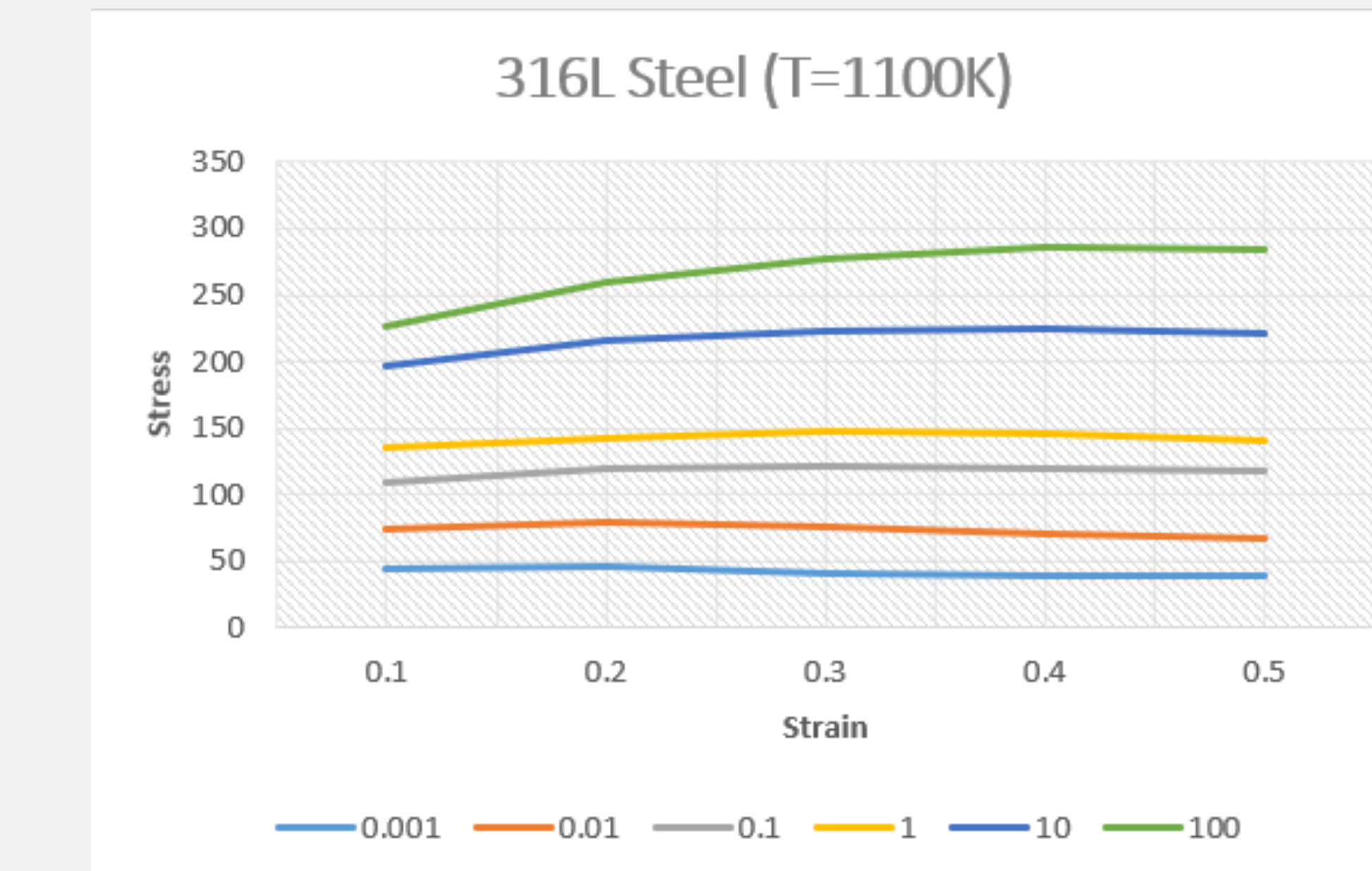
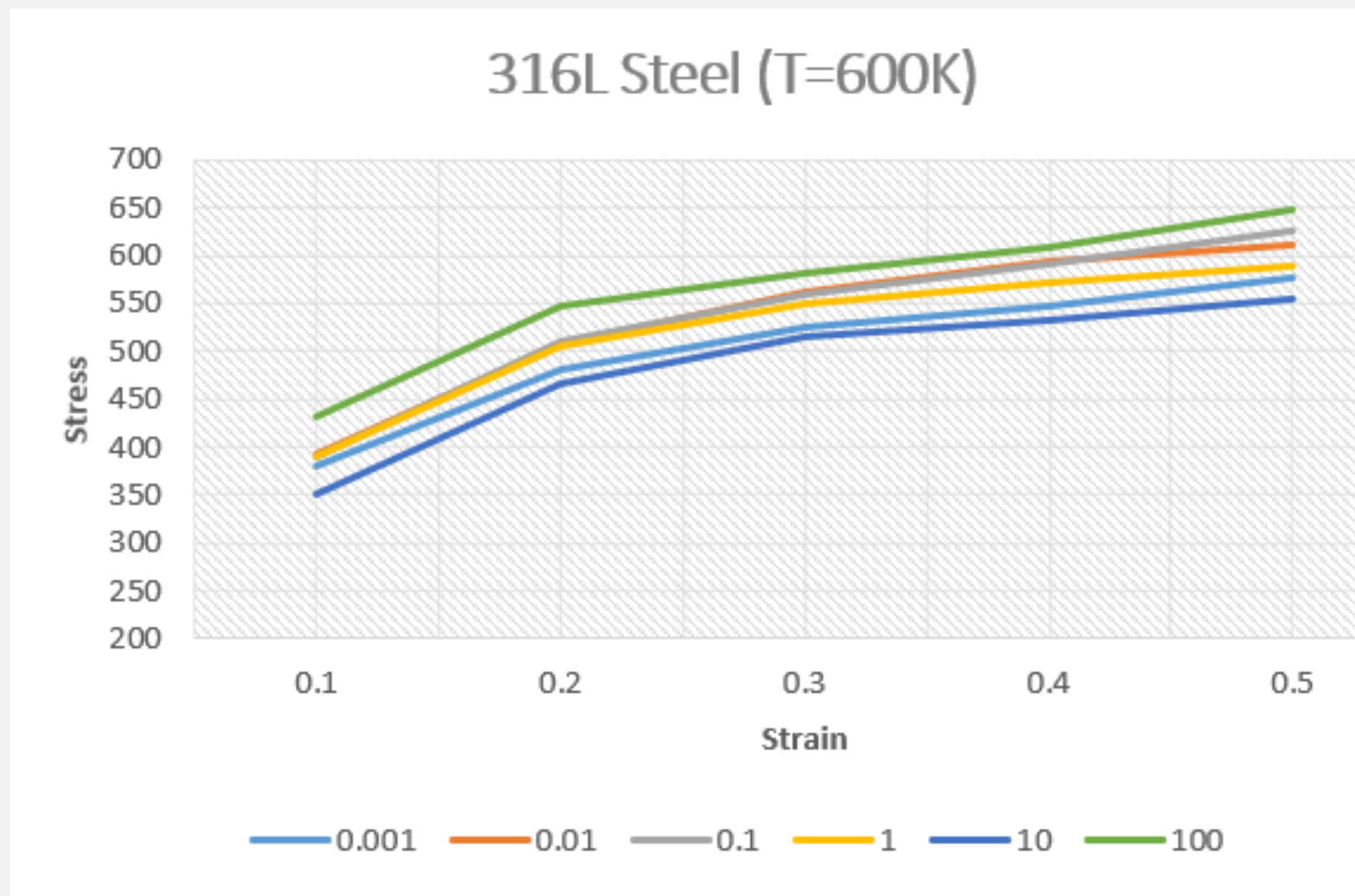
316L STAINLESS STEEL

- Stainless steel type 316L is extensively used for high temperature applications where creep resistance is an important consideration. The alloying element that imparts high temperature strengthening to this stainless steel is molybdenum.
- The addition of Molybdenum retards the recovery and recrystallisation process, lowers the hot ductility, increases the rolling and extrusion loads, and causes considerable solid solution strengthening at elevated temperatures.
- In this experiment, the sample used has the following **composition**:

Cr-18.6, Ni-11.6, Mo-2.3, Mn-1.7, C-0.02, S-0.007, P-0.04, Si-0.77, Fe-bal.

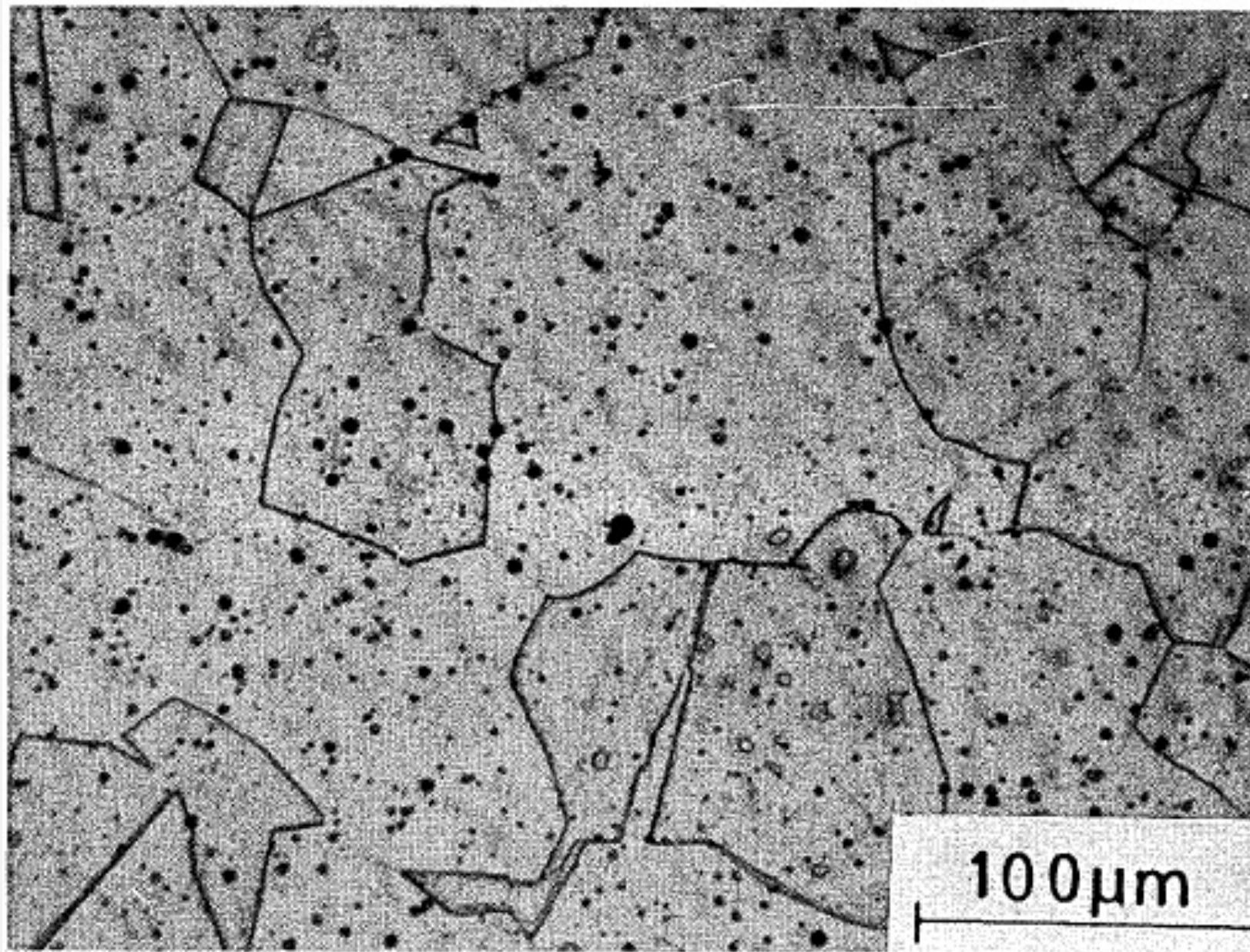
FLOW STRESS VS STRAIN FOR DIFFERENT STRAIN RATES

- The Stress vs Strain curves recorded are as follows:

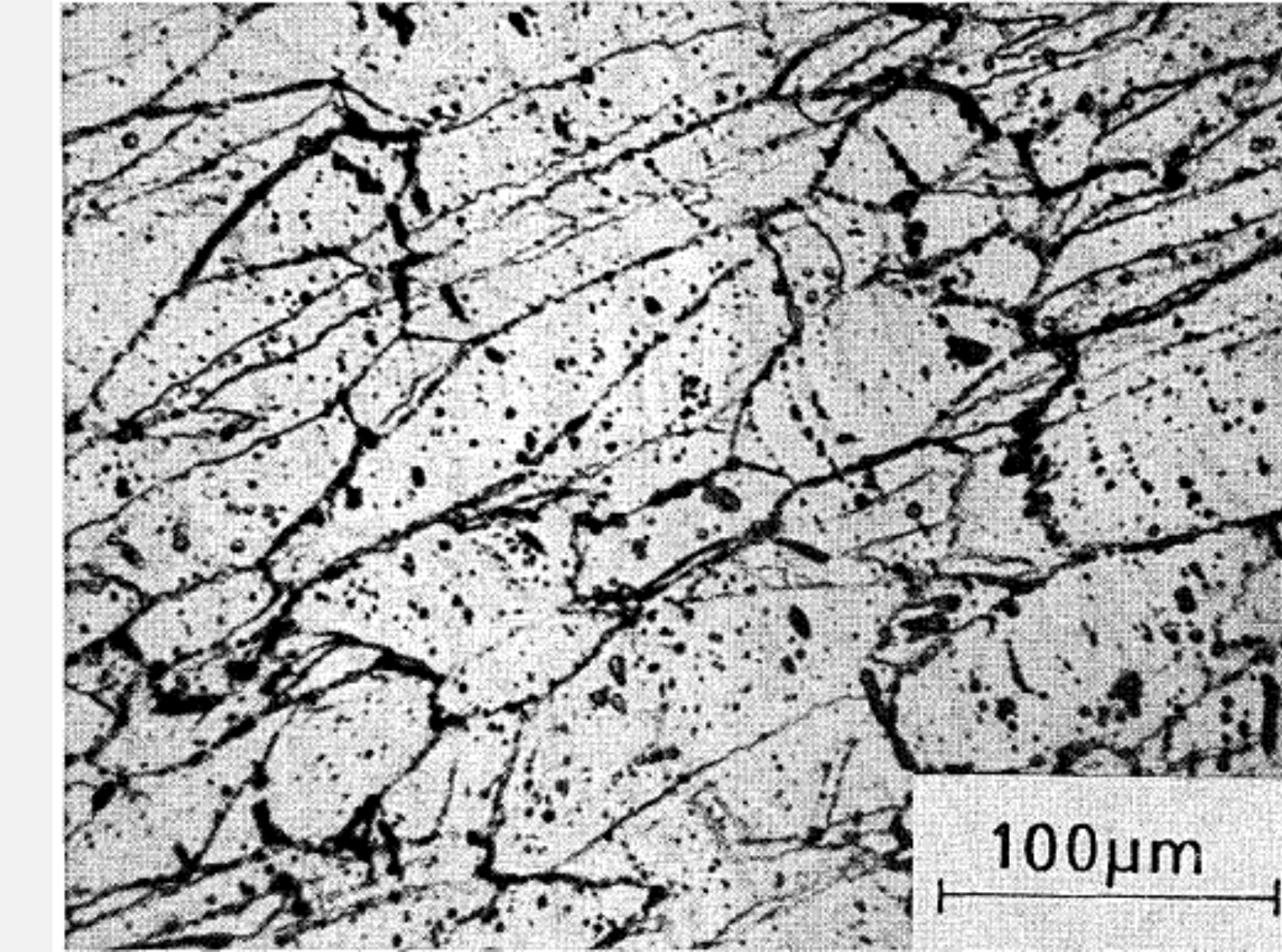


We get to know that the behaviour of graphs is different for the two regions : $T < 1000K$ & $T > 1000K$. At temperature lower than 1000K, the curves exhibit typical behaviour whereas at temperatures greater than 1000K, we see that the flow stress attains a peak at a critical strain and reaches a steady state at higher strains.

MICROSTRUCTURAL ANALYSIS

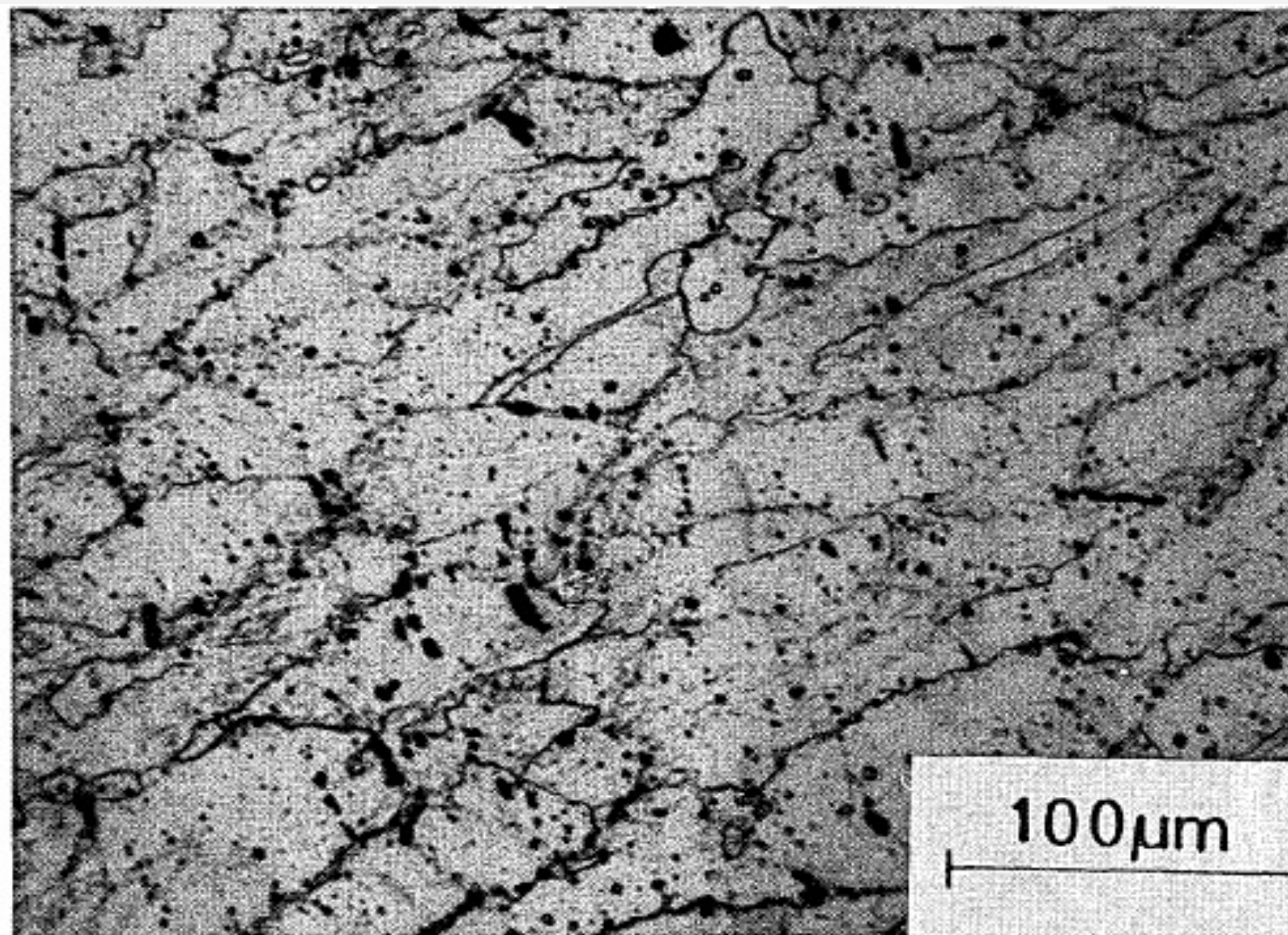


Initial microstructure of 316L steel used for hot compression tests.

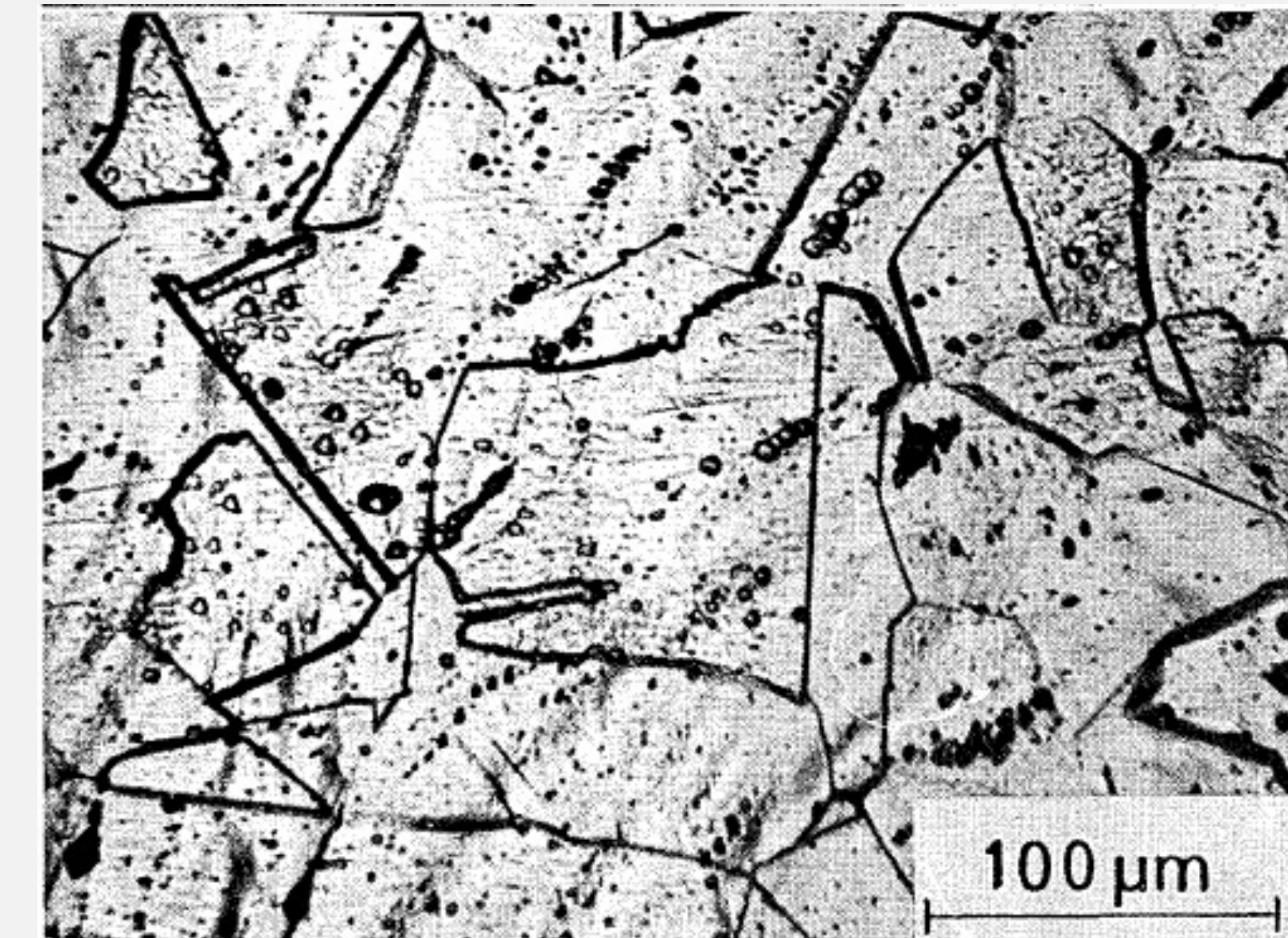


Sample deformed at temperature 900°C and strain rate 0.001 s⁻¹. This here is a typical dynamically recovered microstructure.

MICROSTRUCTURAL ANALYSIS



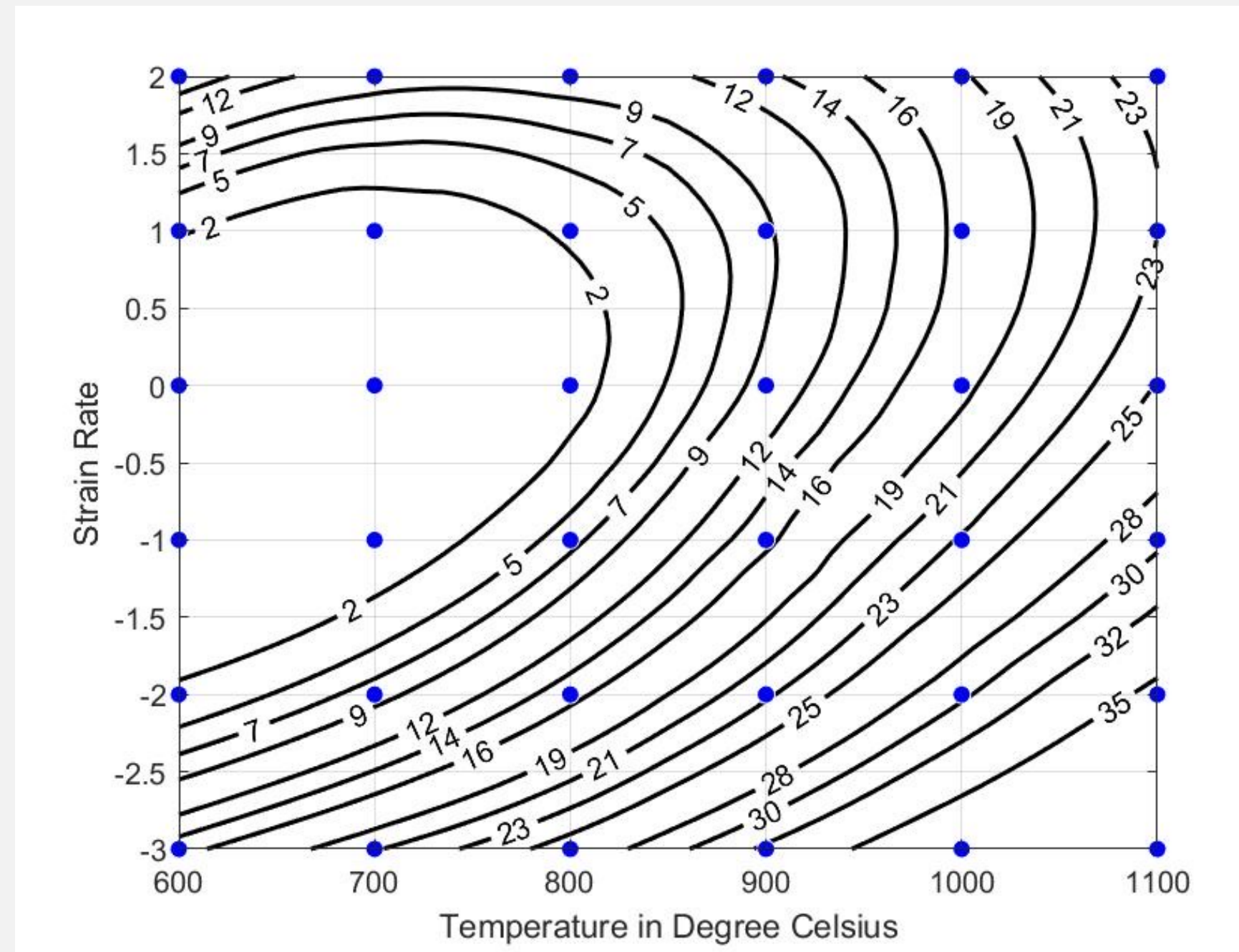
Sample deformed at temperature 1000°C and strain rate 0.001 s^{-1} . The presence of corrugated grain boundaries here suggest that DRX has started.



Sample deformed at temperature 1200°C and strain rate 0.1 s^{-1} . This here is a completely recrystallised microstructure.

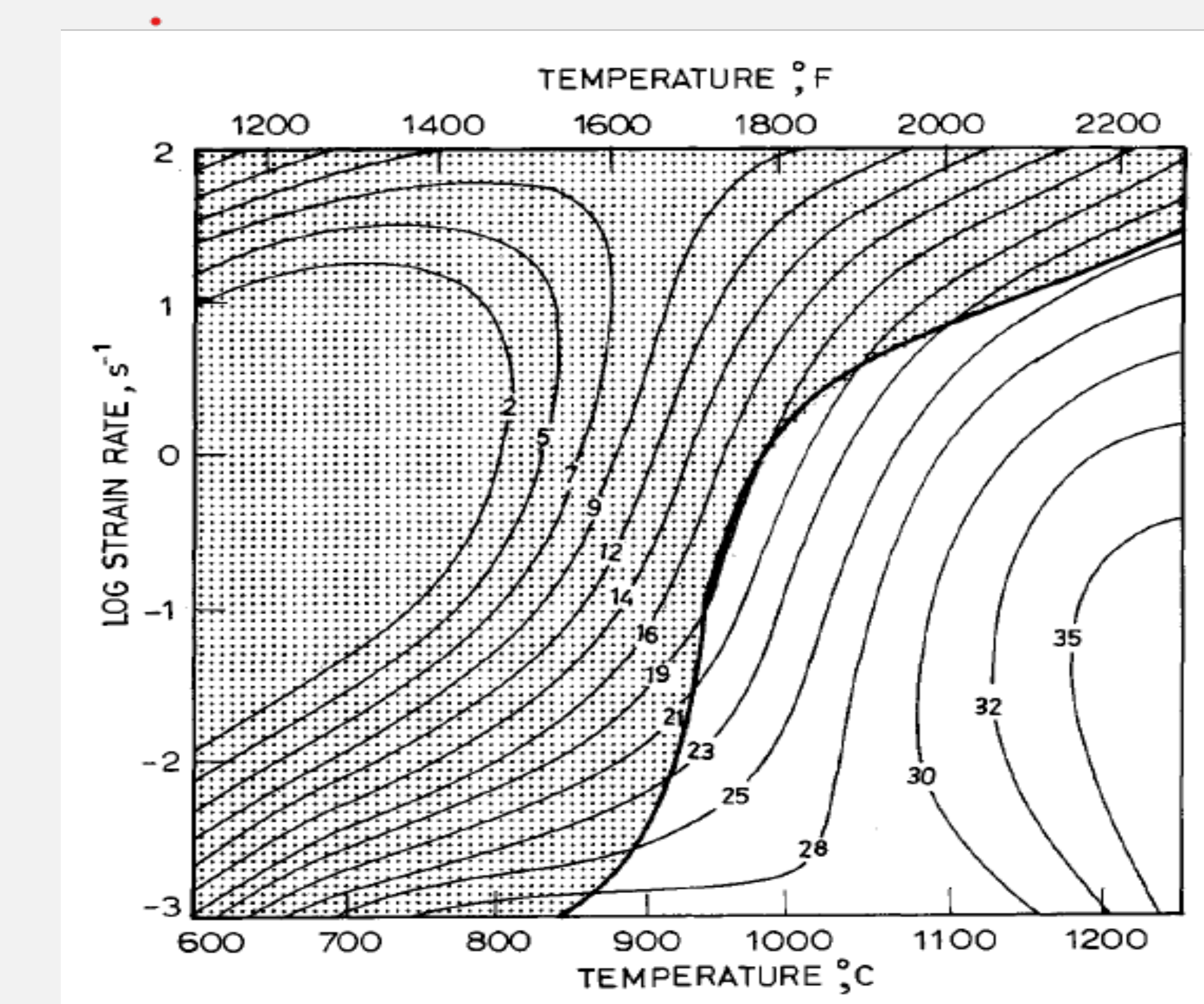
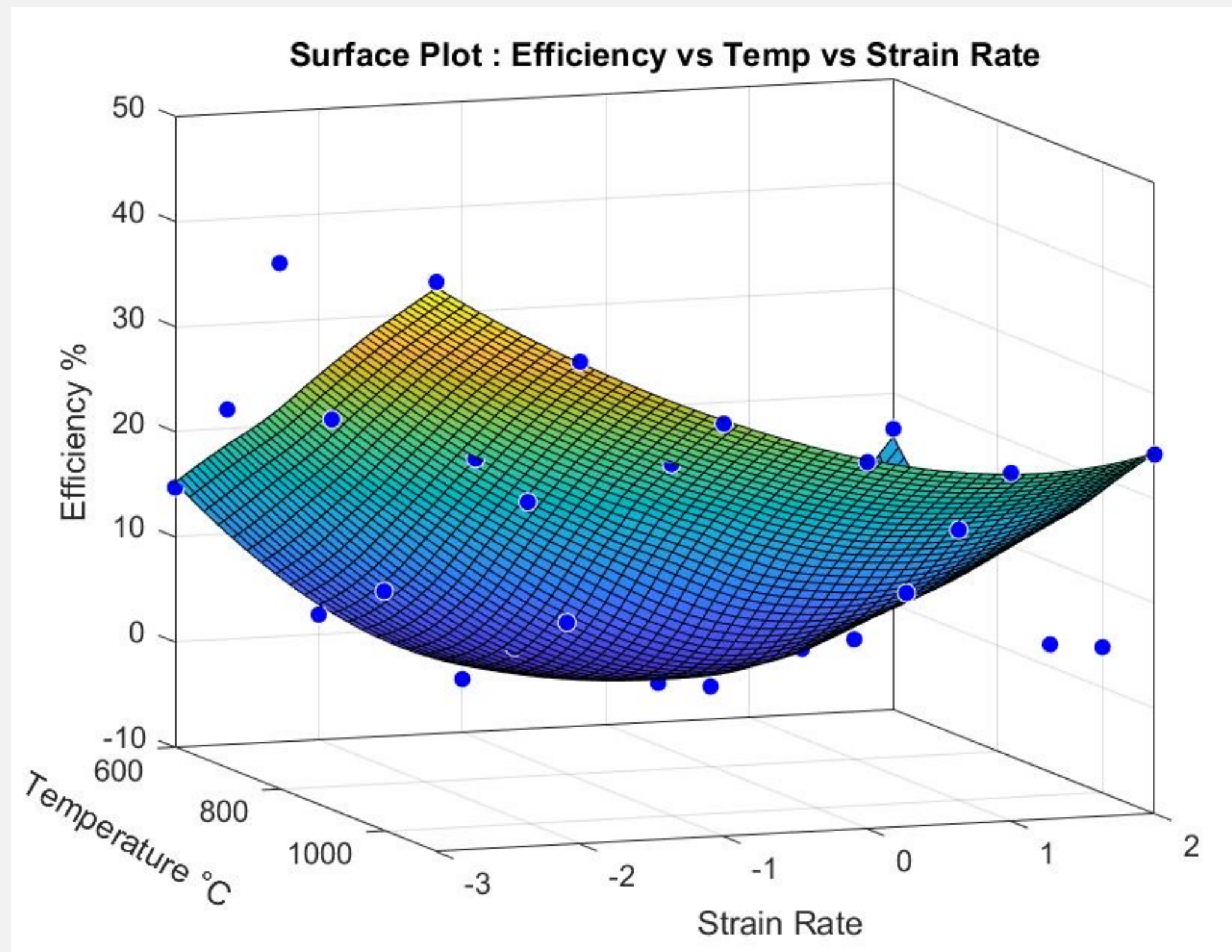
MAPS

- The power dissipation map of the sample at strain 0.5 is shown below:



- The plot here reveals two different domains :
 - in the range 1000-1250 °C and 0'001-10 s⁻¹.
 - at 750-1000 °C and 0'001-0'01 s⁻¹ with a peak efficiency of 28 % at 900 °C and 0.001 s⁻¹.

PROCESSING MAPS



The processing map plotted for strain 0.5 in 3D as well as 2D .

CONCLUSION

- Stainless steel type AISI 316L undergoes dynamic recrystallisation with a peak efficiency of 35% at 1250°C and 0.05 s^{-1} , which are the optimum parameters for hot working.
- The material undergoes dynamic recovery at 900°C and 0.001 s^{-1} .
- Three distinct regions of instabilities have been observed. At temperatures lower than 850°C and strain rates lower than 10 s^{-1} , flow localisation has occurred. · At higher temperatures and strain rates, mechanical twinning and wavy slip bands are observed. At temperatures $<850^{\circ}\text{C}$ and strain rates $>10 \text{ s}^{-1}$, intense adiabatic shear bands are formed. All these regimes must be avoided in processing AISI316L.

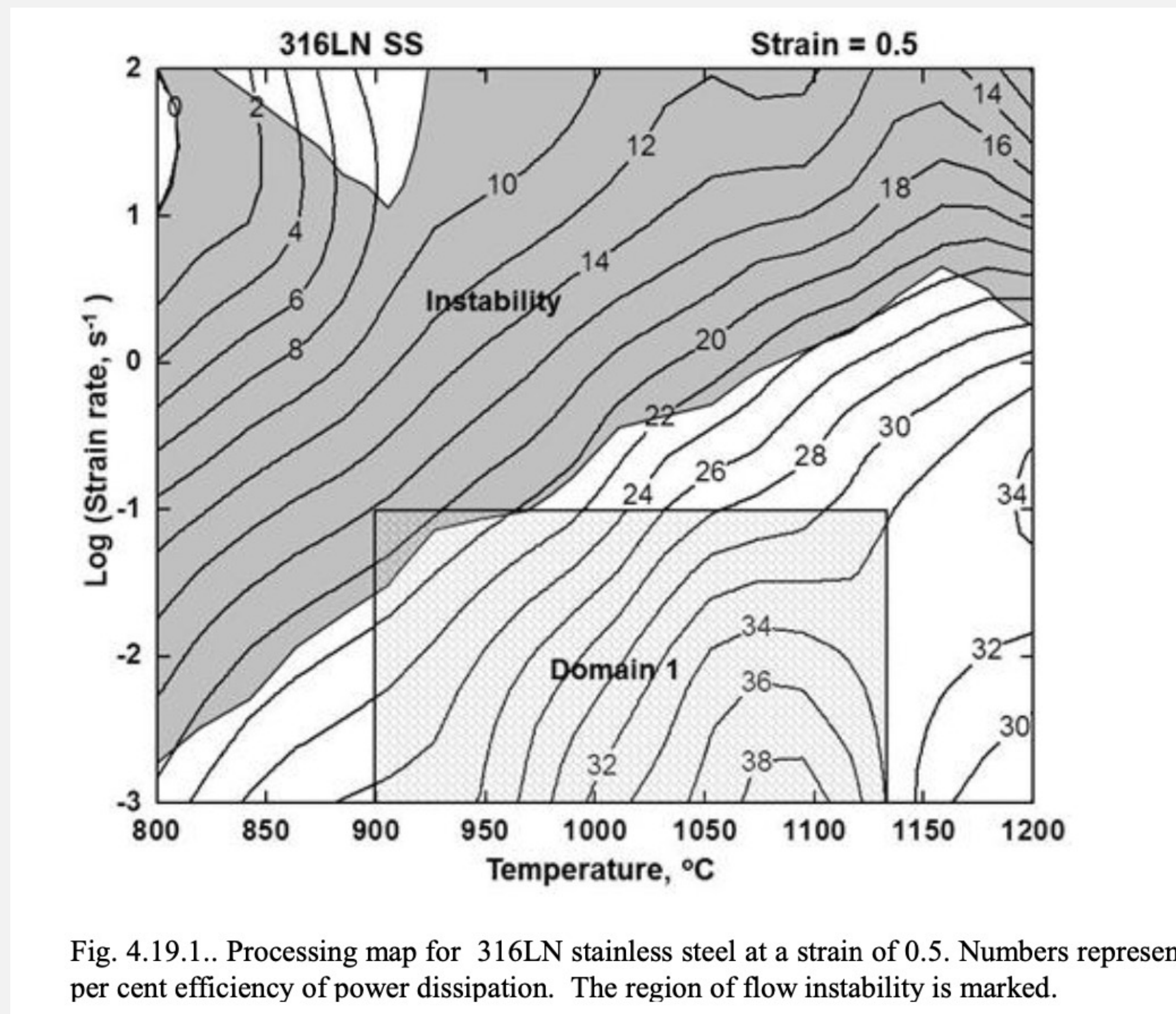


316LN-STAINLESS STEEL

316LN-STAINLESS STEEL

- **Material** - AISI 316 low carbon nitrogen strengthened stainless steel
- **Composition** - 16 – 18 Cr, 11 - 14Ni, 2 - 3 Mo, 0.02 – 0.03 C, 0.1 – 0.16 N, 0.8 – 1.5 Mn, 0.3 – 0.7 Si, Fe - Bal
- The 316LN has low carbon content and uses nitrogen instead of carbon as an austenite stabilizer and solution hardener.
- Low carbon in this stainless steel prevents stress corrosion cracking.
- The steel is strengthened by increasing nitrogen content.
- However, the presence of nitrogen causes dynamic strain ageing at lower temperatures (200-700C) and can reduce the ductility.
- Hot deformation behavior of this steel as well as that containing Nb is studied using **Gleeble Machine**.
- DRX occurs in the temperature range 1050 - 1200 and lower strain rates.

Processing Map of 316LN Stainless Steel

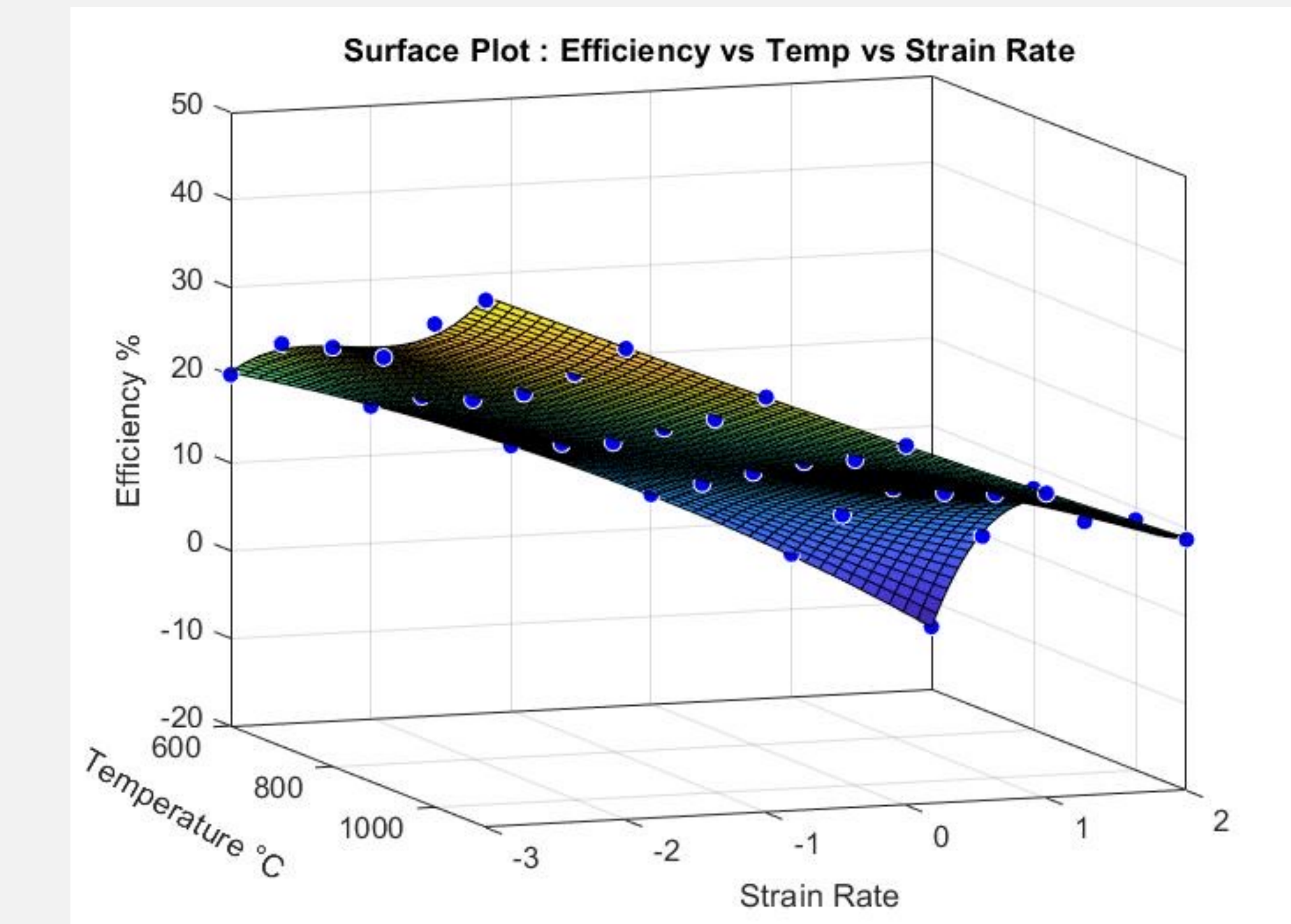
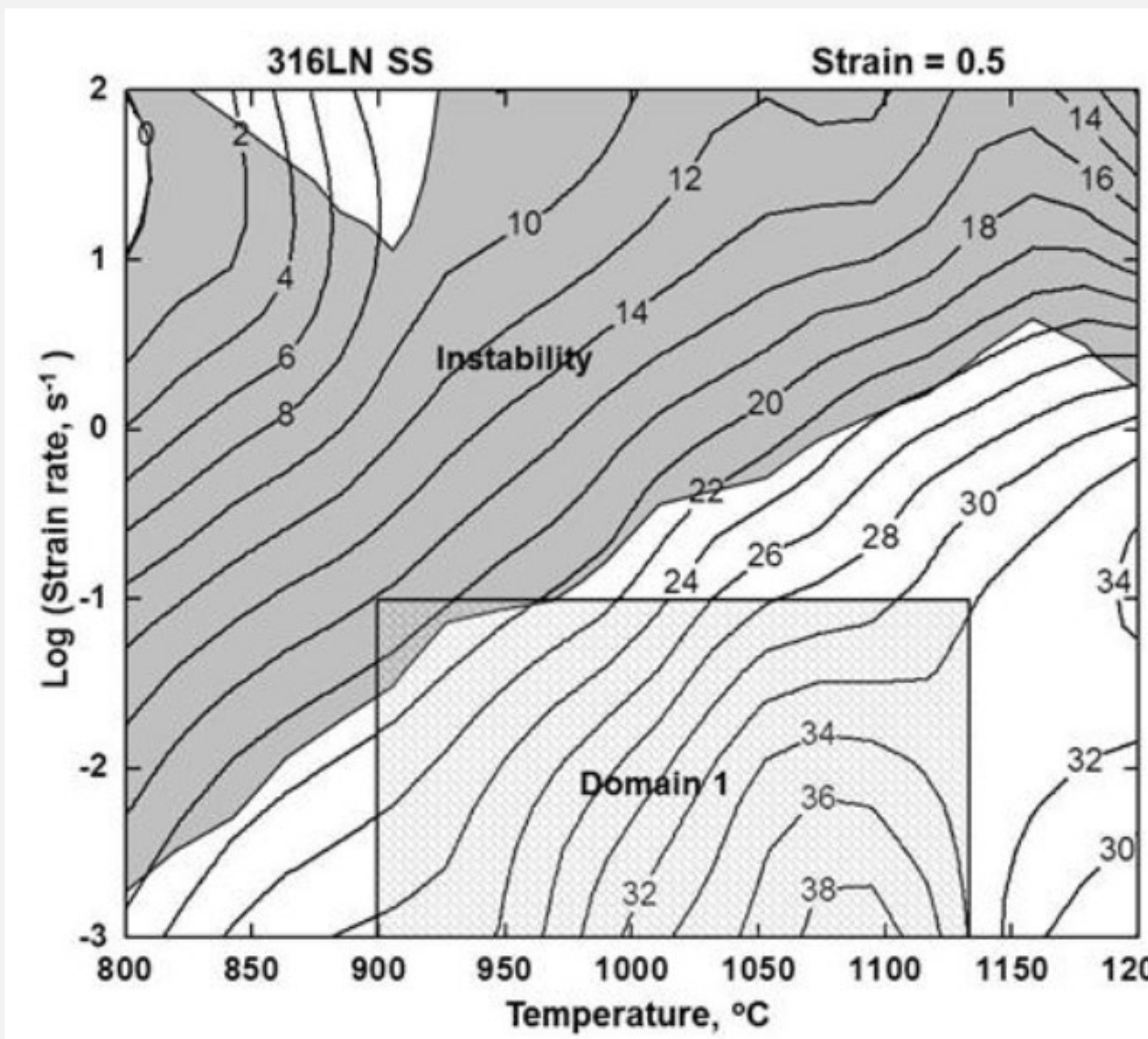


- The processing map exhibits a **single domain** in the temperature range 900 – 1125°C and strain rate range 0.001 – 0.1 s⁻¹; with a peak efficiency of 38% occurring at 1100°C and 0.001 s⁻¹.
- The steel exhibits **cracking along the adiabatic shear bands** at temperatures in the range 800 – 850 C and at strain rates higher than about 3 s⁻¹
- The material also exhibits a wide range of **flow instability** extending to lower strain rates at lower temperatures and higher strain rates at higher temperatures. The manifestation is flow localization.

Metallurgical Interpretation and Processing Conditions

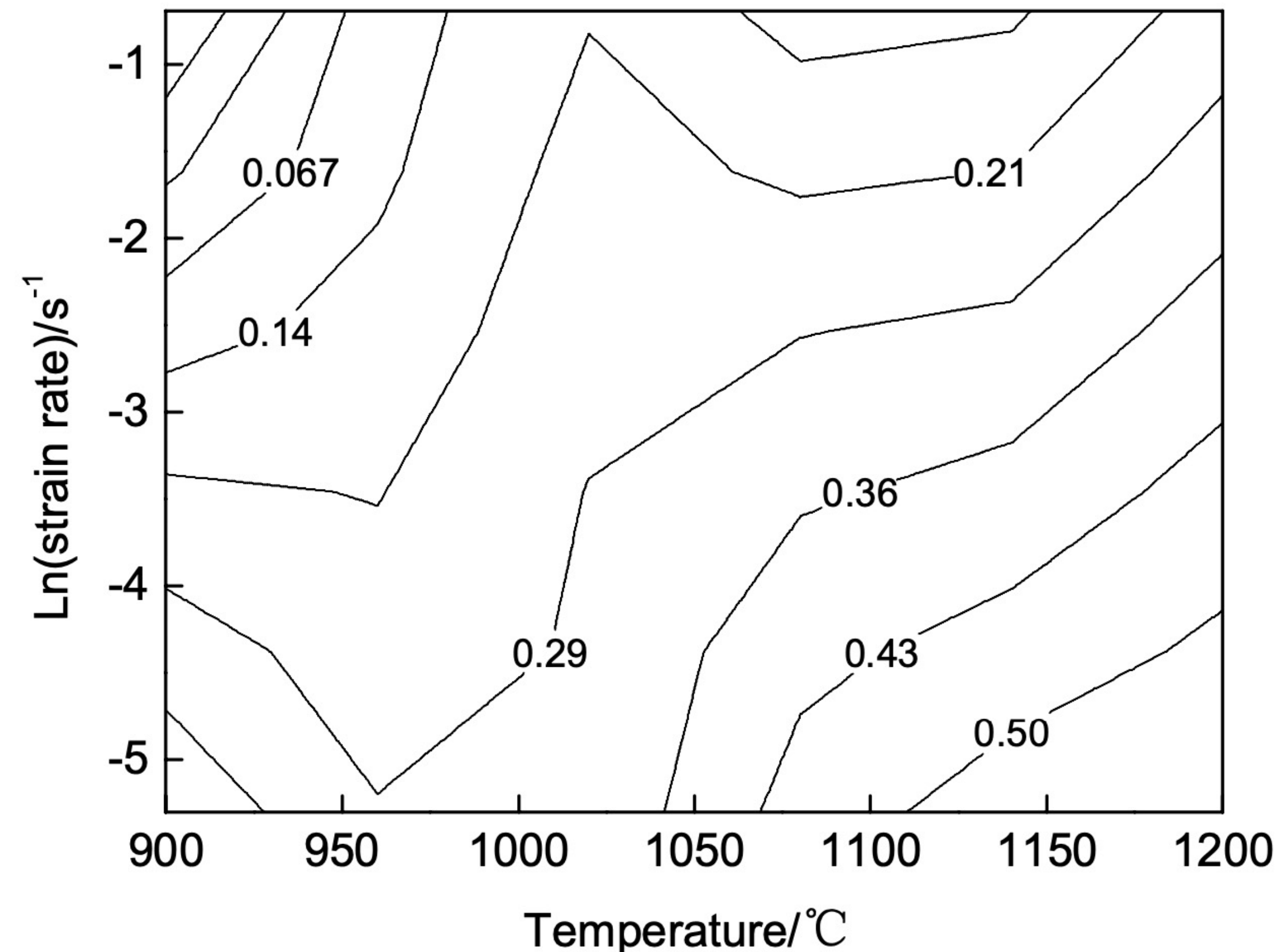
Manifestation	Temperature, °C	Strain rate, s⁻¹
Dynamic recrystallization	900-1125	0.001-0.1
Cracking along adiabatic Shear bands	800-850	> 3
Instability	800-1000 1000-1200	>0.1 >1
<i>Optimum Conditions:</i> <i>1100 oC and 0.001 s⁻¹</i>		

PROCESSING MAPS OF 316LN STAINLESS STEEL



The processing map plotted for strain 0.5 in 2D as well as 3D .

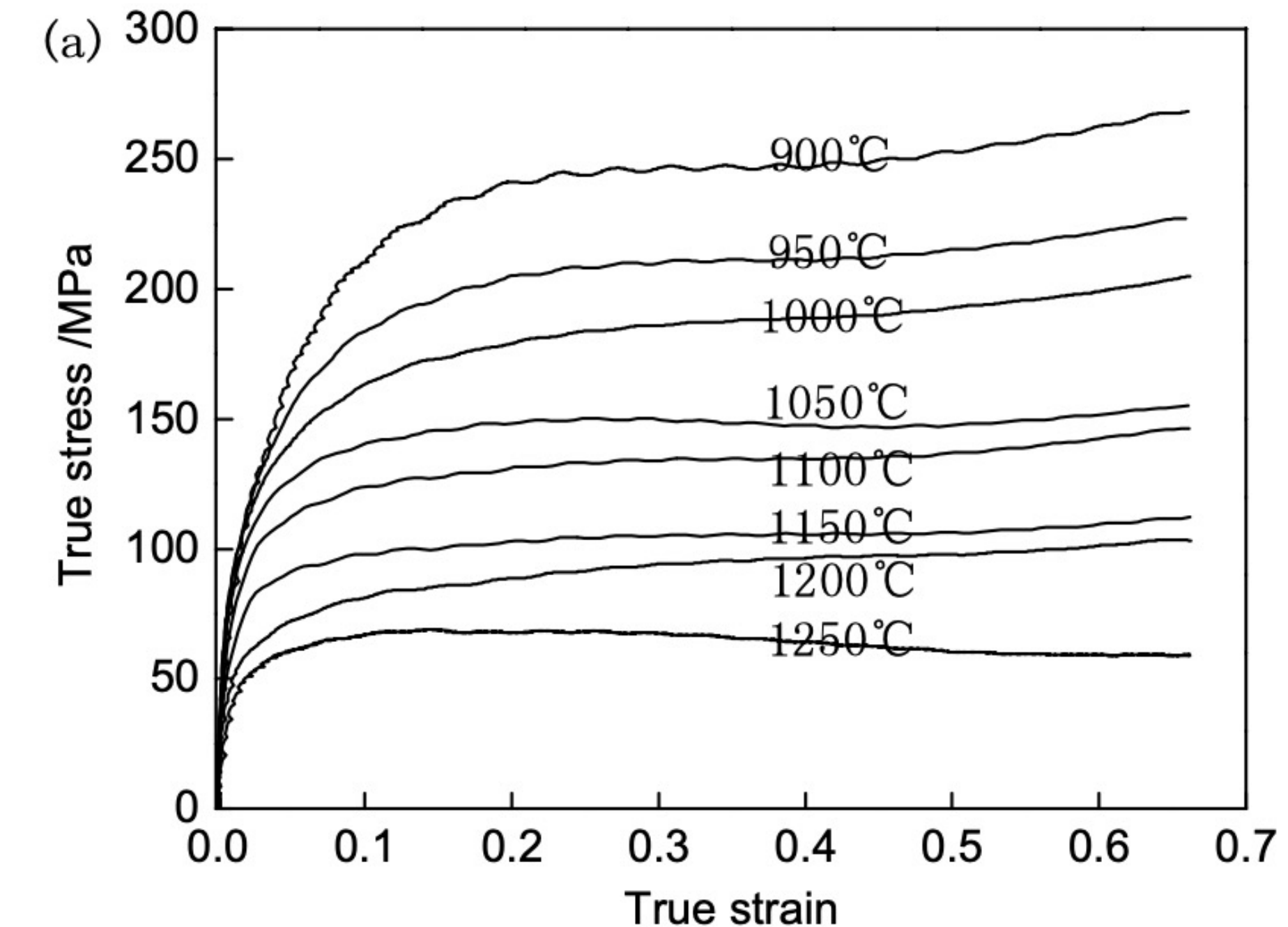
ISO-EFFICIENCY MAP OF 316LN STEEL.



- It is found that when strain rate remains the same, power dissipation rate increases with rising deformation temperature;
- When temperature remains the same, power dissipation rate increases with decreasing strain rate.
- The maximum rate is 0.50 emerging at nearly $1100\text{--}1200^{\circ}\text{C}$ and 0.005s^{-1} . The minimum rate is 0.067 emerging at $900\text{--}950^{\circ}\text{C}$ and 0.5s^{-1} .
- INTERPRETATION:
Larger power dissipation rate is observed at $1050\text{--}1200^{\circ}\text{C}$ and lower strain rate which indicates dynamic recrystallization may happen.

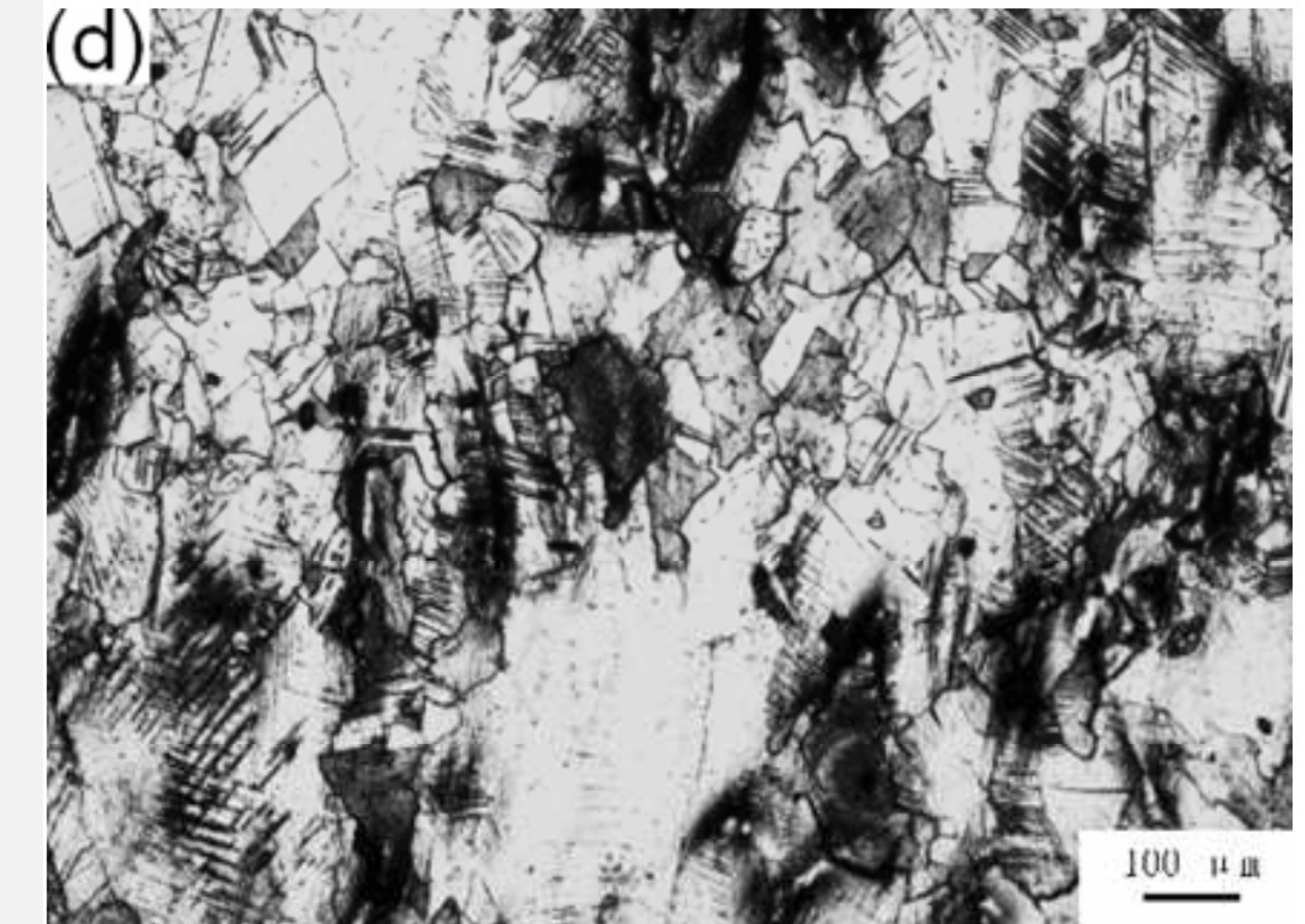
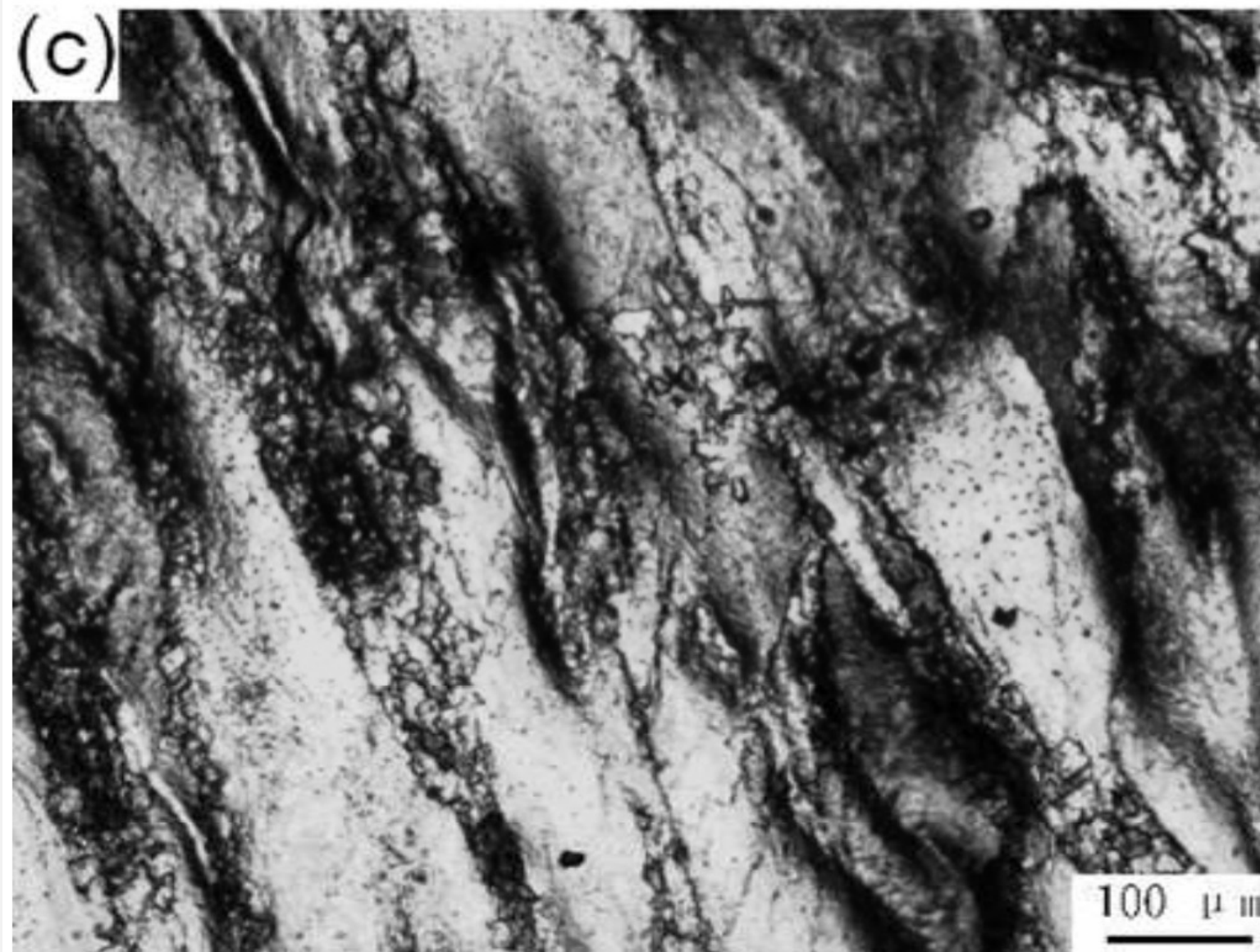
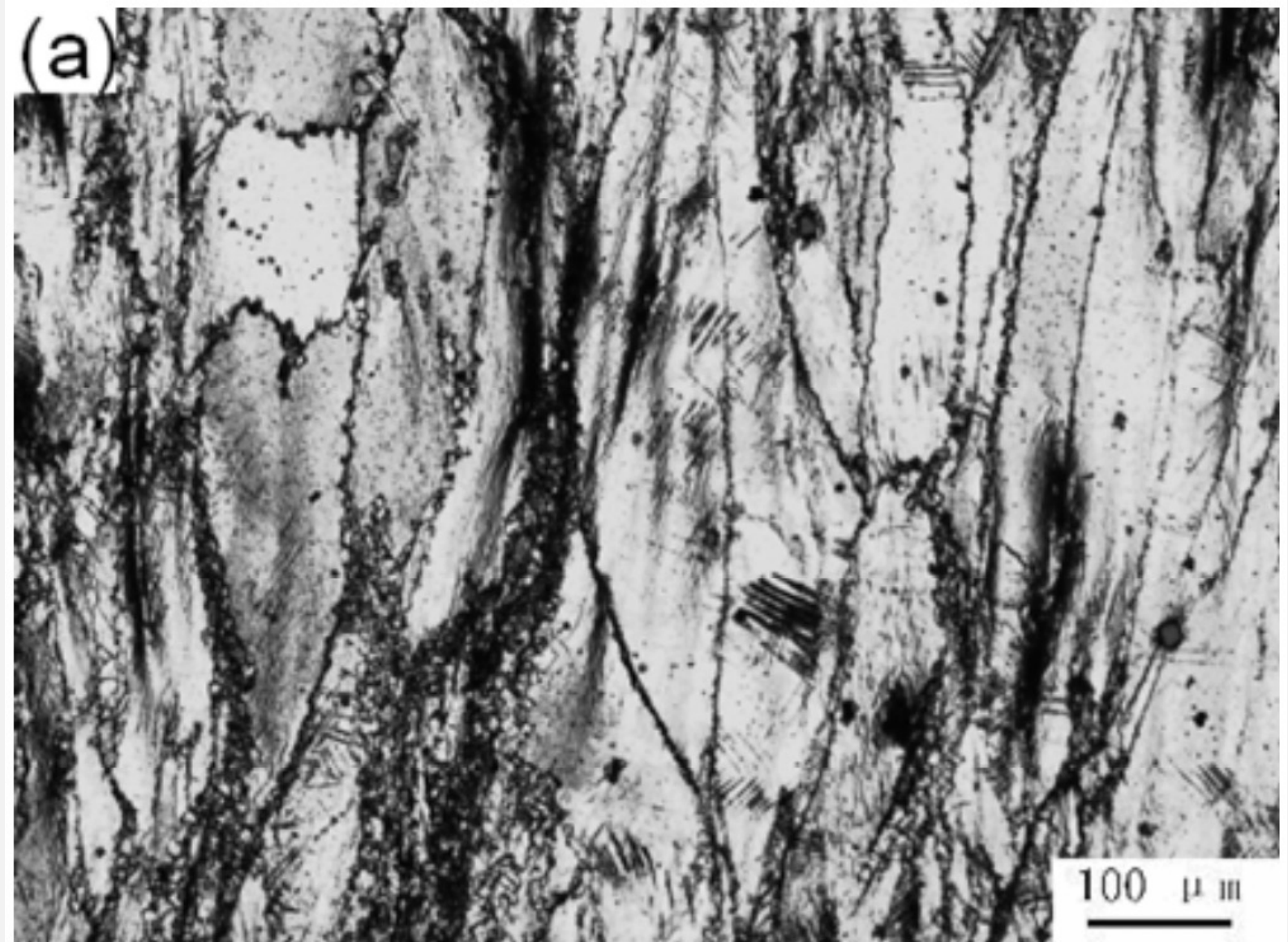
EXPERIMENTAL RESULTS AND DISCUSSION

- The true stress-strain curves of 316LN stainless steel are presented
- This shows the effects of deformation temperature on the flow behaviour of 316LN steel.
- If strain rate remains the same (0.5 s^{-1}), flow stress generally decreases with the rise of deformation temperature.



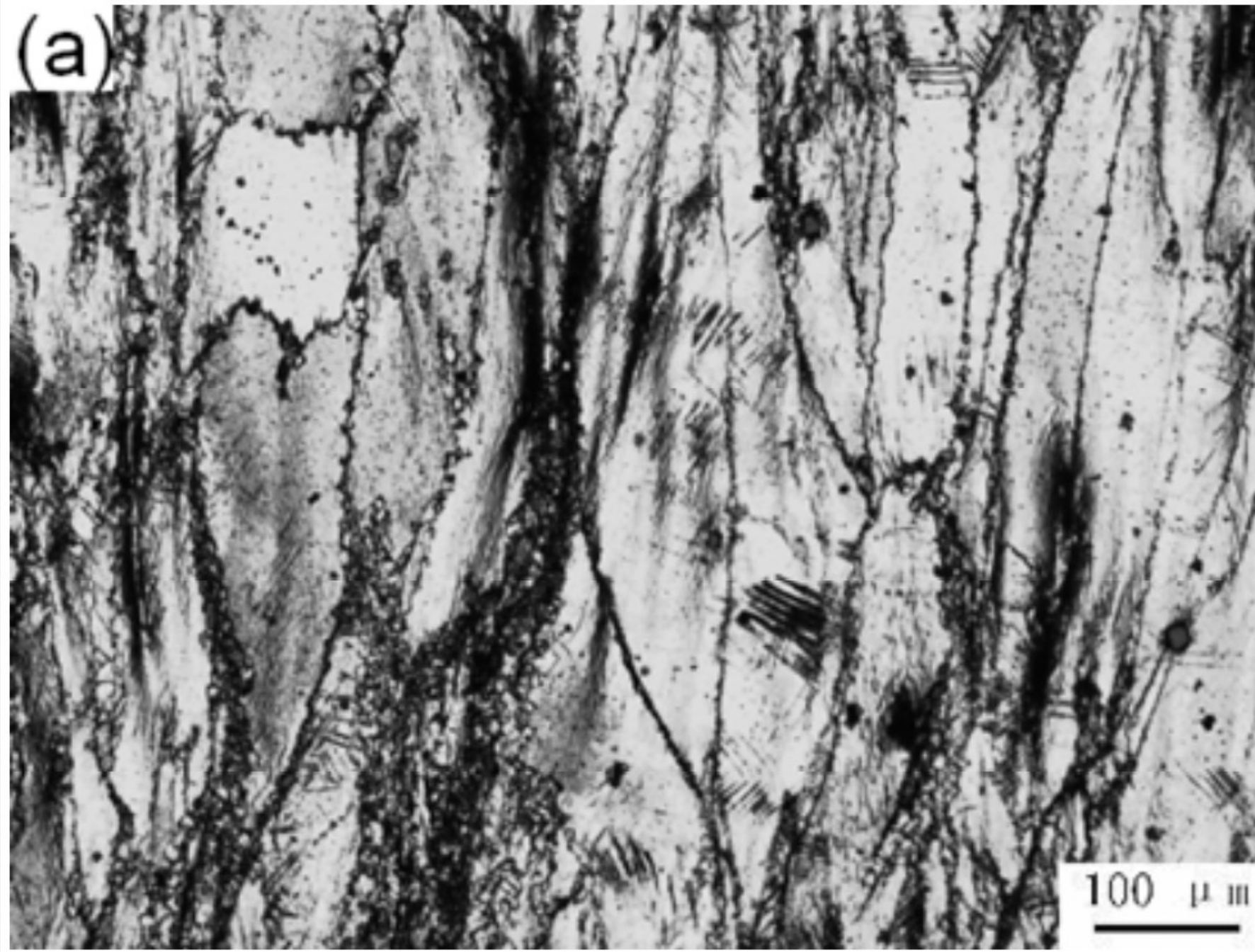
MICROSTRUCTURE EVOLUTION OF 316LN STEEL.

Effect of different temperatures



Effect of strain rates

- 316LN steel undergoes the dynamic recovery
- Elongated grains become distinct with the increasing strain rate
- This is because that the grains do not have enough time for recovery at larger strain rate.



(A) At 900°C, 0.005s⁻¹

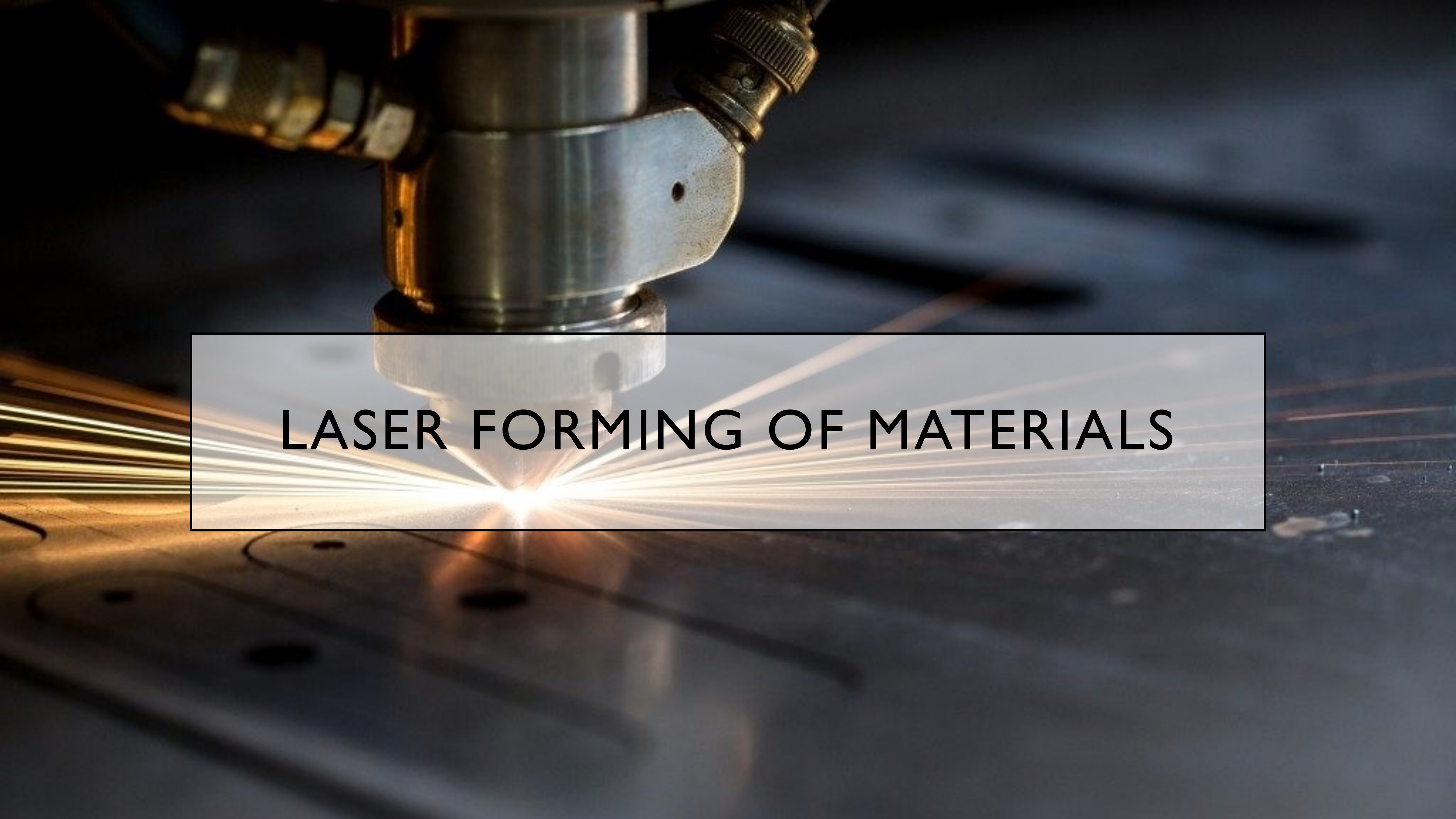


(B) At 900°C, 0.5s⁻¹

FACTS

- Stainless Steel was originally called **Rustless Steel.**
- Stainless Steel history - On 17 October 1912, [Krupp](#) engineers Benno Strauss and Eduard Maurer patented as **Nirosta** the [austenitic stainless steel](#) known today as **18/8** or AISI Type 304.





LASER FORMING OF MATERIALS

INTRODUCTION

The “LASER” acronym stands for Light Amplification by Stimulated Emission of Radiation.

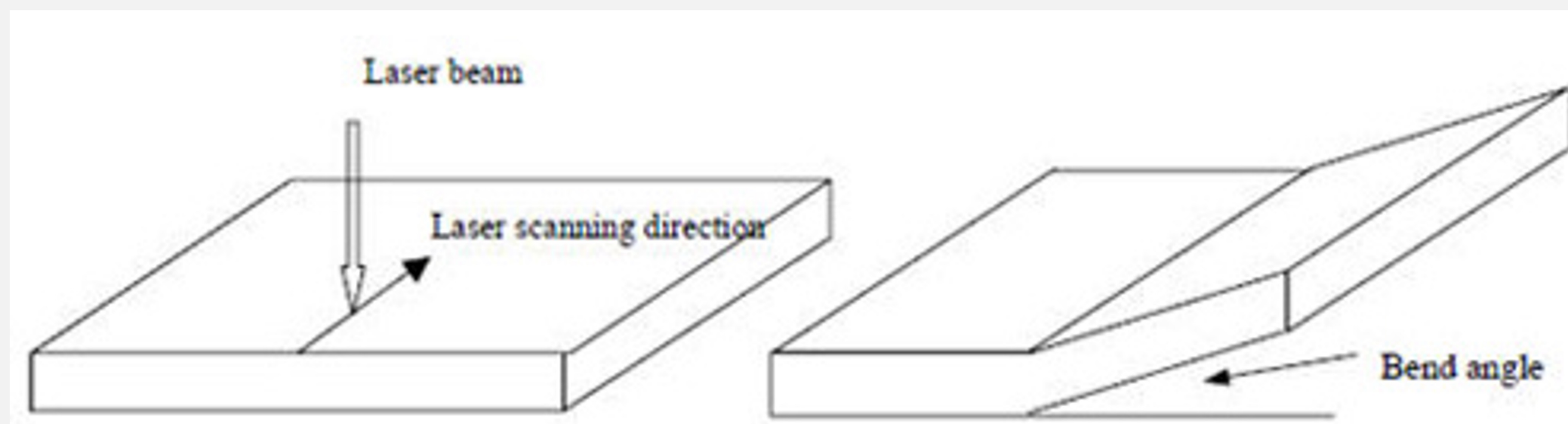
Theodore H. Maiman built the first laser in 1960 at Hughes Research Laboratories.

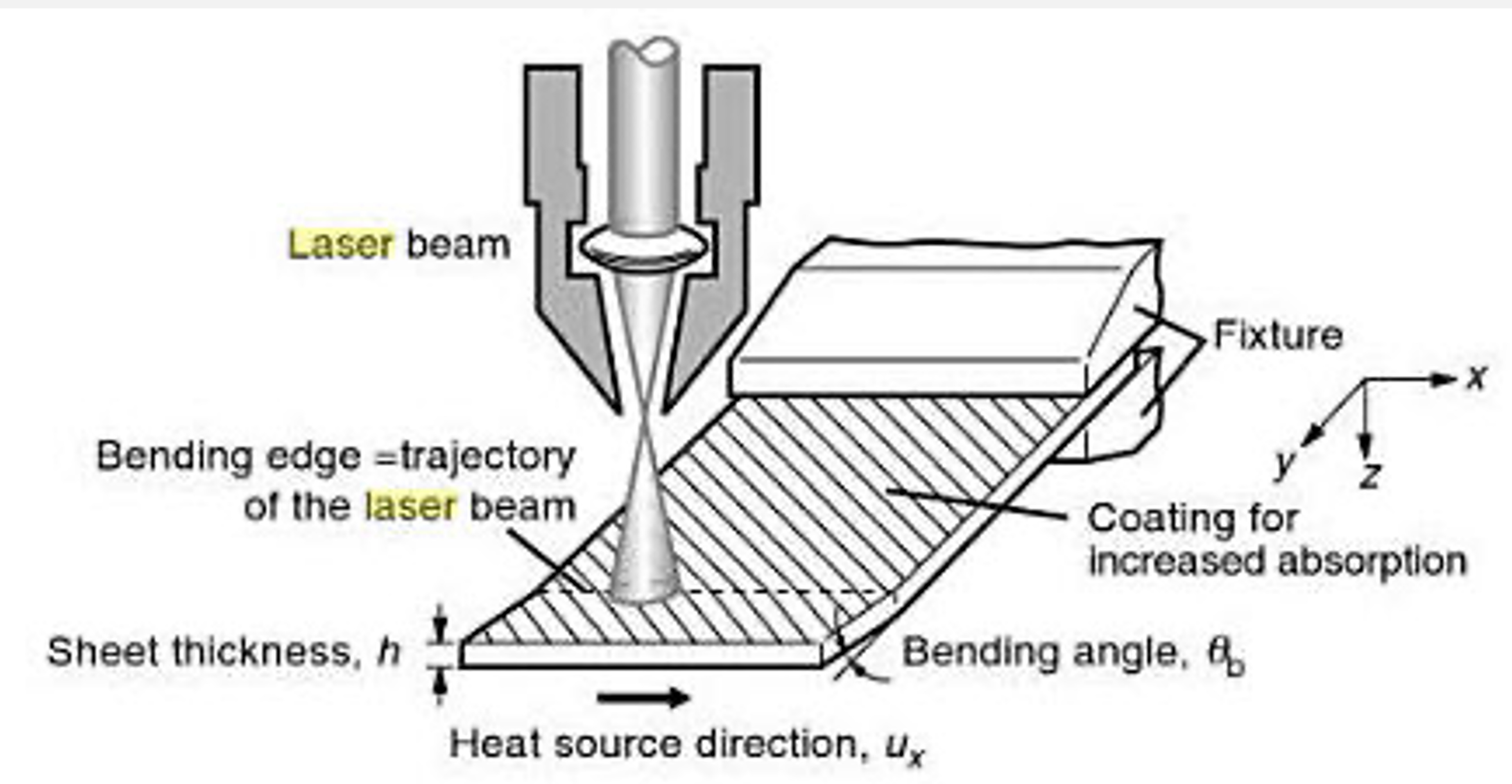
Laser forming (LF) uses laser-induced thermal distortion to shape sheet metal parts without hard tooling or external forces. It is a highly flexible rapid prototyping and low-volume manufacturing process.

Laser beam irradiation induces thermal stresses into the worksheet.

The cooling of the sheet leads to bending the sheet due to residual stresses and corresponding strains.

By increasing the temperature during laser beam irradiation, the physical properties of the sheet - yield strength, ultimate tensile strength, and the elastic (Young's) modulus will also be decreased.





ADVANTAGES:

- The cost of the forming process is greatly reduced because no tools or external forces are involved in the process.
- Because this process is a non-contact forming process, precise deformation can be produced in inaccessible areas.
- The size and power of the laser beam can be precisely manipulated, enabling accurate control of the forming process and improving reproducibility.
- Laser forming uses localized heating to induce controlled deformation instead of tradition entire work piece heated. Therefore it has the advantage of energy efficiency.
- Laser forming is suitable for materials that are difficult to form by mechanical approaches.

APPLICATIONS:

Simple examples of parts produced by laser forming method are beverage containers, angle brackets, or connecting rods. Thermo-mechanical forming, however, enables parts (sheet metal, rod, pipe, or shell) to be formed without external forces and does not require the use of dies.

Laser forming has potential applications in aerospace, shipbuilding, microelectronics, automotive industries, etc. Examples of Laser formed parts are given in the figure.



LASER BENDING OF MONOLITHIC SHEETS

Sheet bending is a vital manufacturing process which can be performed using laser technology. The sheet is scanned along a straight line, and local heating of one of the sheet's surfaces leads to the plastic deformation of the sheet due to the stress gradient over the thickness direction.

The process parameters affecting the bend angle are laser characteristics (laser power, spot size, scan speed, pulsed or continuous irradiation), the number of irradiation passes, material type, and the geometrical dimension of the sheet (thickness, width, length).

LASER BENDING OF BI-LAYER AND TAILORED BLANKS

Different properties of the sheet can be obtained by increasing the number of layers (bi-layer sheets or multilayer sheets), manufacturing a composite sheet, or different thickness or material (tailor welded blanks (TWB), tailor machined blanks (TMB)).

Tailor-made blanks are sheet metal assemblies with different thicknesses and/or materials and/or surface coatings. The laser melts the sheet, and bending happens due to plastic deformation during solidification. The thickness affects the bending angle. Different thicknesses, start point of scan and absorbed power by the sheet (laser power and scanning speed) influence the bending magnitude of the TMB sheet.

LASER FORMING OF COMPOSITE SHEETS

The composites are divided into three categories, polymer matrix composite (PMC), ceramic matrix composite (CMC), and metal matrix composite (MMC).

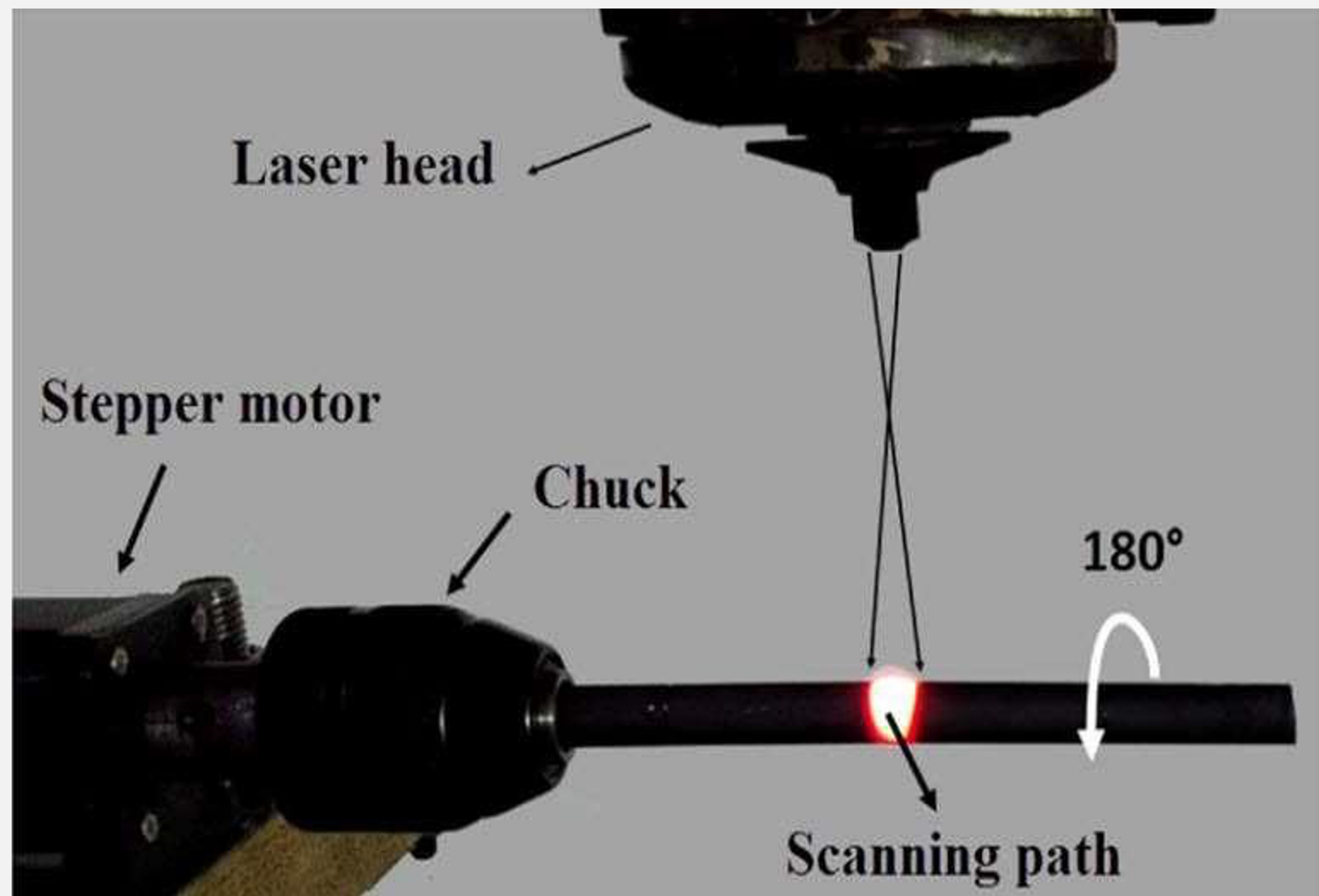
Fiber and matrix have different mechanical properties (yield strength, stress-strain behavior) and physical properties (melting point, density, conductivity).

Fiber–Metal Laminates (FML) are made of different layers of metal and composite material. The difference between the properties of fiber, matrix, and metal leads to complicated plastic deformation, bending, and unpredictable.

LASER TUBE BENDING

- . Tube bending was always a challenge in conventional bending. Usually, an internal plug is inserted inside the tube, and bending happens. However, a laser beam can also be used for tube bending. The laser beam is irradiated on the tube surfaces and may result in 2D or 3D tube bending.
- . The effects of the irradiating length and the number of irradiating passes on tube bending have been studied. Three primary defects of the laser tube bending are lateral bending angle (especially when the scanning path is complicated like spirals), ovality, and thickness variation. The tube bending angle increased by increasing the irradiation length and number of passes. Moreover, the ovality percentage and the thickness variation will be increased by increasing the irradiation length.

- . The effect of process parameters is like sheet metal forming, and the bending angle of the tube increases by increasing the laser power and beam diameter and with a decrease in the travel speed.
- . Laser beam absorption can also be performed to improve the obtainable bending angle. Different materials, such as carbon steel, stainless steel, and nickel tubes, can be formed and used in various industries such as aerospace industries, engines, heat exchangers, and air conditioners.
- . The size of the tube is another essential process parameter. Normal sizes, such as $\frac{1}{2}$ and $\frac{3}{4}$ inch tubes, can be formed using a laser beam without difficulties. However, the laser forming of micro-tubes (for example, a tube with 635 μm outer diameter) needs more precise tools and controlled conditions



OPTIMIZATION

- . The selection of process parameters is crucial in laser forming. A comprehensive analytical model which determines the bending angle of the sheet during laser forming has not been derived until now. This is mostly due to the complicated nature of laser forming.
- . In this way, statistical tools are powerful tools for finding the effect of process parameters and determining the behavior of the sheet during laser forming. Full factorial design of experiments, response surface methodology, fuzzy logic strategy, Particle Swarm Optimization (PSO), Artificial Neural Network (ANN), Taguchi approach, Genetic Algorithm (GA), and other statistical tools are implemented to derive an equation for prediction of bending angle.

- . The number of process parameters for laser forming is high, and studying the effect of process parameters is not possible experimentally. So, in most studies, a finite element analysis using commercial FEM codes is verified by experimental tests and the other set of experiments simulated by FEM.
- . For example, Omidvar et al used the Taguchi orthogonal design of experiments (four factors-five levels) to find a maximum bending angle for a 1 mm thick AA6061-T6 sheet. Twenty-five experiments had been carried out to find the maximal bending angle of 28.7° .
- . The aim of the Taguchi method, in which the robust control of parameters leads to less uncertainty in the fabricated workpiece.
- . The optimal condition is determined according to the least-cost plating methodology (LCPM) to reduce the number of passes and use the highest laser power. Moreover, a combination of fuzzy logic controller and particle swarm optimization (PSO) methods is proposed by the researchers to find the proper set of input parameters to catch a predefined bending angle.

DOUBLY CURVED PARTS

- . The laser beam irradiation path is an important parameter that can be used for shaping complicated parts including bowl-shaped surfaces, cylindrical surfaces, saddle-shaped surfaces, and intricate 3D shapes
- . different scanning paths like spiral movement, concentric circles, crossed lines, spider pattern movement, and other developed scanning strategies make a complicated plastic strain field in the sheets and form the sheet to the desired shape.
- . Kant et al used a curvilinear path for forming of thick and thin sheets. The results show that the bend angle increases with a decrease in scanning path curvature in thick sheets.
Different scanning paths can be utilized for the fabrication of curved parts

Reference	Fabricated Shape	Irradiation Scheme
Chakraborty et al	Bowl-shaped surface	Radial scan
Liu and Yao	Pillow and saddle shaped surface	Calculated paths
Na and Kim	Saddle-shaped surface	Calculated paths
Gao et al	Ship hull shape	Calculated paths
Imani Shahabad et al	Dome-shaped surface	Spider scanning paths
Shen et al	Pillow,warped and saddle shape	Computational scanning path

CONCLUSIONS

This review has briefly described the most remarkable and recent developments in laser-forming technology and applications involving single-layer, multilayer, and composite sheets. Topics covered include sheet bending by laser beam irradiation, tube bending, optimization of process parameters, Doubly-curved parts have an essential role in the shipbuilding and aerospace industries and were discussed in a separate section. The laser beam technology can be used more creatively to fabricate special parts, such as saddle-shaped surfaces or the bending of micro-tubes. The experiences of the authors show that developing analytical solutions can help researchers to fabricate simple bending, but analytical solutions are not effective enough to manufacture accurate and complicated shapes. Combining numerical methods, statistical approaches, and experimental knowledge can be a proper solution for the manufacturing of intricate shapes.

REFERENCES:

- [Recent Advances in the Laser Forming Process:A Review](#)
- <https://www.totalmateria.com/page.aspx?ID=CheckArticle&site=kts&NM=260>
- <https://encyclopedia.pub/entry/3094>
- Identification of flow instabilities in the processing maps of AISI 304 stainless steel -S.V.S. Narayana Murty, B. Nageswara Rao,* , B.P. Kashyap
- Hot Working Guide—A Compendium of Processing Maps, Y.V.R.K. Prasad, K.P. Rao, and S. Sasidhara, editors
- Modelling of hot deformation for microstructural control –Y.V.R.K Prasad and T Seshacharyulu
- Processing Maps:A Status Report -Y.V.R.K. Prasad (Submitted 19 September 2003)
- Processing Map for hot working of Stainless steel type AISI 316L –Y.V.R.K Prasad, SL Mannan, S Venugopal
- Dynamic Softening mechanisms in 304 austenitic stainless steel -N. D. Ryan and H. J. Mcqueen
- Hot Working Characteristics Of Steels In Austenitic State - H.J. McQueen, a S.Yue,b N.D. Ryana and E. Frya
- Processing maps for hot working of commercial grade wrought stainless steel type AISI 304 -S.Venugopal and S. L. Mannan
- Hot Deformation Behavior of 316LN Stainless Steel - Wenwu HEa, Jiansheng LIUb, Huiqin CHENa, Huiguang GUOa